

Chapter 1. Introduction

This thesis presents a new GIS tool that predicts GPS satellite visibility for an entire test area for a given day and time period. The tool is named *Satellite Viewsheds* and is unique in its ability to consider line of sight obstructions between a GPS receiver and the satellites; obstructions that may cause loss of or reduced service. No such tool currently exists. This chapter offers the GIS and GPS concepts employed by this research, and includes a discussion of the following project objectives:

- 1) Research the current availability and capabilities of existing GPS satellite visibility prediction tools and determine if there is an existing method of performing predictions considering features of a local environment
- 2) Address the anticipated incapability of existing tools by creating a new GIS tool to perform GPS satellite visibility predictions for any place and time while considering possible signal obstructions
- 3) Assess the performance of the new tool with a field test

1.1 Geographic Information Systems

A Geographic Information System (GIS) is a complex computer software system that is used for the management, storage, display, and analysis of spatial data. GIS developed along with the evolution of mapping from manual data entry and management, as it had been done for thousands of years, into the digital world. This transition began as early as the 1960's, with the developments of primitive computer mapping systems such as SYMAP at the Harvard Laboratory (Carstensen, 2003). Although the line-printer maps produced by SYMAP were crude by today's standards, its development opened the

door for an explosion in the usage of computers for mapping. Perhaps the most prolific period of enhancement to computer mapping technologies has occurred over the past two decades and is arguably continuing today, with the advent and growth of present-day GIS. GIS has become an immeasurably powerful tool for the display, management and analysis of geospatial data and is now used extensively by the intelligence community, local and federal governments, environmental agencies, planners, developers, and researchers worldwide. The GIS software used in this research was ArcGIS version 9.0, produced by Environmental Systems Research Institute, Inc., or ESRI, a well-known heavyweight of GIS software. More specifically, the computer program written for this research runs in ArcMap, ESRI's window-oriented display and analysis GIS product.

Two primary models of geospatial data are used in a GIS: vector and raster. Vector data are used to represent exact points in space. These points can be used by themselves as point vector data, or may be connected to form line or polygon vector data. Vector data is used to represent discrete features such as roads, streams, and political boundaries. Although useful for many applications in GIS, vector data was not used in this research. This project focuses on raster data. Raster data consists of rectangular cells of equal size, and a raster grid is a set of rows and columns of cells. Each cell, or pixel, has a single value that is uniform across that cell. Raster data is used to model continuous data such as elevation and temperature.

Although raster grids can be used to represent many types of data, *Satellite Viewsheds* uses a surface model grid to perform its satellite visibility analysis. A surface

model is a raster grid in which the cell values hold a height or elevation attribute. One of the most commonly used surface model grids is the Digital Elevation Model (DEM), in which each pixel contains a representative elevation of the space on the earth's surface that it represents. A sample DEM is shown in Figure 1. The DEM was obtained from the United States Geological Survey's (USGS) seamless data FTP site at

<http://seamless.usgs.gov/>. While DEMs can be useful for raster surface analysis with their multitude of available cell sizes, DEMs represent the "bare earth". DEMs do not include buildings, vegetation, or other items that may obstruct the line of sight (LOS) between a GPS satellite and its receiver. There are, however, other types of surface models that include possible LOS obstructions in addition to bare-earth terrain. One such model is a Light Detection and Ranging (LiDAR) image. LiDAR is an active form of remote sensing that records the travel time of light pulses emitted by and returned to an aircraft to accurately measure surface elevation in a relatively small geographic region. LiDAR records the elevation data of both bare-earth and surface features such as vegetation and structures. *Satellite Viewsheds* will accommodate both DEM and LiDAR

grids, as well as any other raster surface model grid. The type of grid used to test the tool was actually an appended elevation model, with building heights added to an elevation grid of the Virginia Tech campus (see Chapter 3).

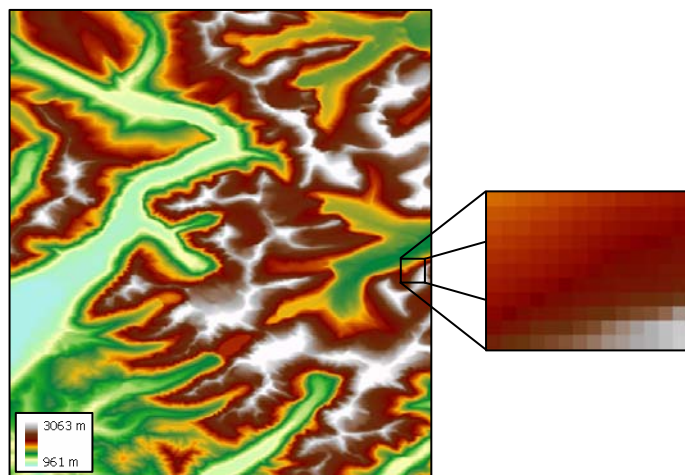


Figure 1. Sample DEM of central Glacier National Park, Montana, at a resolution of 15 m. The inset shows a close-up of individual cells.

1.2 Hillshades and Viewsheds

Many types of manipulation and mathematical operations can be performed on raster surface model grids. This research focuses on two specific types of raster analysis: the hillshade and viewshed. Hillshades and viewsheds and their relevance to GPS satellite visibility will be explained in detail in Chapters 2 and 4, but this section provides the basic concepts. Both hillshades and viewsheds involve the analysis of a raster surface model grid. The aim of a viewshed is to determine those parts of a landscape that can be seen from a given point or set of points (Burrough, 1998). In other words, a viewshed uses the features of the terrain to determine whether each pixel in a surface model grid can establish LOS with the given source point(s), which are located somewhere on the grid. Figure 2 shows an example of a viewshed using the Glacier DEM, with the three points representing the view source points. The term “viewshed” may also be used to

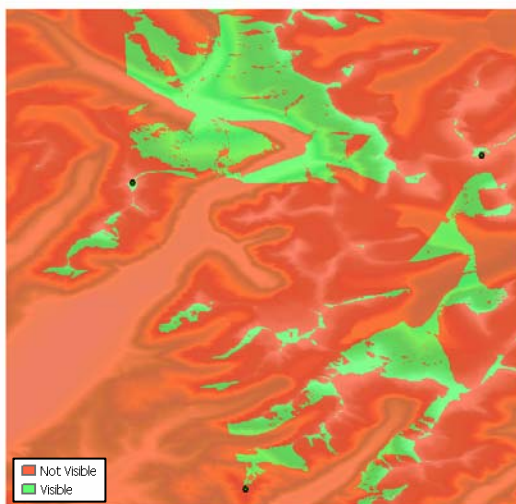


Figure 2. An example of a viewshed; performed on the Glacier DEM using the three points as view

describe a region of visibility from a source point. Throughout this paper, the term viewshed will most often be used to describe an area of visibility as opposed to describing a GIS operation. Viewsheds may be used in applications such as the determination of the optimal location for a fire watchtower or the least visible location in which to place a landfill.

A hillshade, on the other hand, is often used for display rather than analytical purposes. In a hillshade, there is one imaginary light source that is somewhere in the sky and assumed to be in the same position relative to each cell in the grid. A hillshade uses the gradient, or degree of change of the plane of a surface, and aspect, the direction in which the cell faces, of each cell in order to assign it a score representing the degree to which that cell is illuminated by the imaginary light source. During display, the cells are often colored, or symbolized, according to this score; creating a mock three-dimensional visualization of the terrain. In ArcGIS, a user has the option to “model shadows” when creating a hillshade. This option treats the imaginary light source as a viewshed source point and creates a grid depicting which cells can establish LOS with the point and which cannot. This concept may be more easily understood if the imaginary light source is thought of as the sun. In this case, a hillshade with shadows modeled would be a map showing those areas that are in sunlight and those that are shaded. Below, Figure 3 shows ArcMap’s Hillshade function user form and output grid, as well as an overlay of the two.

At first glance, it may seem that the current capabilities of hillshade and viewshed operations are sufficient for the prediction of satellite visibility. Although the concepts of each provide the basis for a complete satellite visibility prediction, they cannot complete the task without modification. The shortcomings of each as satellite visibility predictors, as well as an in-depth explanation of their relevance and use in the creation of the new GPS satellite visibility tool, will be provided in Chapter 2.

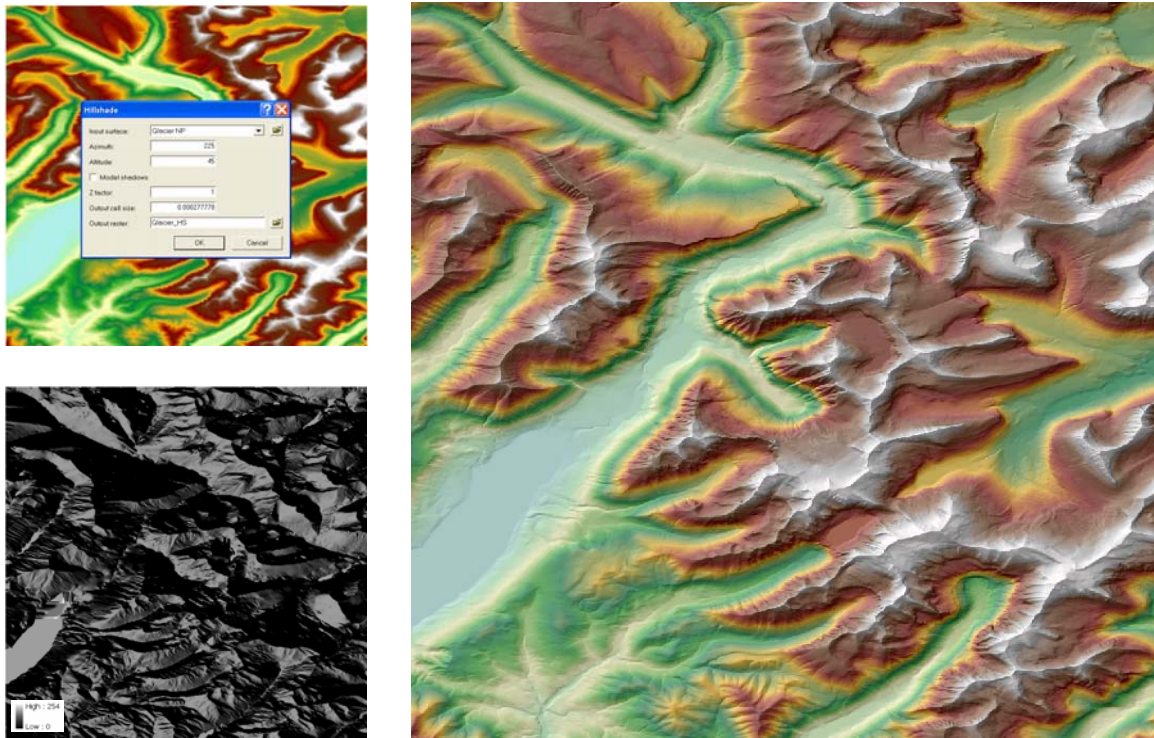


Figure 3. Sample user inputs for ArcGIS's Hillshade command (top left); hillshade grid with cells scored between 0 (shadowed) and 254 (fully illuminated) (bottom left); and overlay of the hillshade and DEM (right)

1.3 Global Positioning System

In recent years, the Global Positioning System (GPS) has developed into the primary navigational and geospatial data collection tool for millions of consumers worldwide. Originally developed in the 1970's by the United States Military and declared open to civilians with "final operational capability" in 1995, GPS uses satellites to provide accurate and rapid positioning information to terrestrial users (Kennedy, 1996). While GIS primarily focuses on the management of geospatial data, GPS is used mainly to obtain geospatial position data.

GPS is comprised of three components. The first segment of GPS is a constellation of twenty-four operational solar-powered, radio transmitting satellites on six orbital planes (Figure 4).

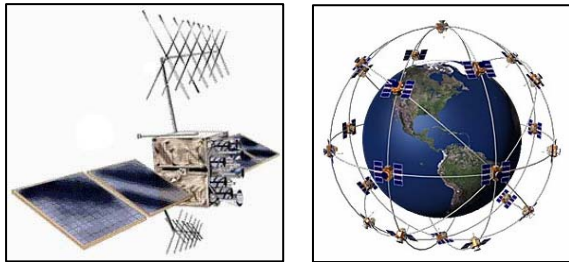


Figure 4. Illustrations of a single GPS satellite (left, courtesy of The Aerospace Corporation) and the GPS constellation (right, courtesy of Garmin)

The satellites are in near-circular orbits at

an altitude of about 10,900 nautical miles above the earth's surface. The satellites' orbits keep them between 60° S and 60° N latitude and the satellites are controlled by several ground stations on the earth's surface, the second segment of GPS. The ground stations monitor both the satellites' on-board electronics and their orbits, which are subject to degradation due to solar wind and gravitational effects of the moon and the sun (Kennedy, 1996). The third segment of the system, perhaps the most familiar to nearly all GPS end users, is the GPS receiver. The receiver is the unit used by a GPS customer for terrestrial navigation, mapping, and geospatial data collection. The unit functions by accepting, or acquiring synchronization with, the radio signals broadcasted from all "visible" overhead GPS satellites at that time. The term visible, in this case, means that there are no obstructions in the line of sight (LOS) between a particular satellite and the receiver and that the receiver is able to acquire the satellite's radio signal. Each signal contains a timestamp indicating when it was transmitted by its parent satellite. The receiver records the exact time at which it receives the signals and calculates the time difference between signal transmission and reception (Δt). Because the speed of the radio signals is known to be 299,792.5 km/s (Kennedy, 1996), Eq. 1.1 can be applied to find the exact distance between each visible satellite and the receiver (Δx):

$$\Delta x = \text{speed} * \Delta t$$

Eq. 1.1

Once the distances to each of several satellites are known, the receiver triangulates its own position, finding the only possible location in which lines of the respective lengths could meet in space. Theoretically, only two satellites are needed to establish the receiver's two-dimensional position and three satellites are needed to establish the three-dimensional position. However, due to the limited precision of the GPS receiver's clock, it requires an additional satellite to synchronize its own clock with the exact time that the satellites are using. Therefore, at least four satellites are required to establish three-dimensional positioning.

The position of a celestial body in the sky relative to a point on the earth's surface is known as the *look angle*. The look angle actually consists of two angles measured from the observer's position, the *elevation angle* and the *azimuth angle*. The elevation angle ranges from 0° to 90° and is measured from a plane tangent to the ground to the point directly above the observer (90°). The azimuth is the compass direction of the spacecraft, measured clockwise from north and ranging from 0° to 360°. To perform visibility analyses for GPS satellites, each satellite's look angle relative to a specified point on the earth's surface must be considered. Given the approximate terrestrial position of a GPS receiver, the orbital properties of the satellites must be determined. From the orbital properties, the look angles can be calculated using the method explained in Chapter 3. *Satellite Viewsheds* requires the orbital characteristics of the GPS satellites in Two-Line Element Set (TLES) format, a popular format used to describe the orbits of

public satellites. Two-line element sets are readily available online and will be described in further detail in Chapter 3.

1.4 Purpose of *Satellite Viewsheds*

The requirement of direct LOS between a GPS receiver and at least four satellites provides the basis for this project. If fewer than four satellites are visible to the receiver, the unit will not be able to calculate its three-dimensional position. Although only four visible satellites are required for a GPS receiver's operation, the accuracy of the position triangulation generally increases for an increased number of visible satellites. For a given receiver, the number of satellites used in the triangulation algorithm is a primary factor in the receiver's performance. The maximum number of operational GPS satellites that a receiver may see at any given time is twelve, although this scenario is rare. It is typically recommended that a receiver use at least six satellites for triangulation, and there are many cases in which this requirement is attained. However, there are also times and locations in which a GPS user's satellite visibility requirement is not met. If the receiver cannot establish LOS with enough satellites, its accuracy diminishes to a two-dimensional (2D) point with an assumed elevation, or it may not function at all. This research focuses on predicting areas and times in which the number of visible GPS satellites is insufficient for a user's objectives.

Due to the dynamic positions of GPS satellites relative to the earth's surface, a GPS receiver's performance varies at different locations and at different times. In many cases, it is important for a GPS user to predict if or how well his or her receiver will

perform during a designated usage time. Current GPS satellite visibility prediction tools perform the analysis under the assumption that the sky above the receiver's position is completely unobstructed. In other words, these tools perform their visibility prediction algorithms without considering LOS obstructions between the receiver and the satellites that may block the signal. The predictions are performed as if the receiver was on "bare earth" or on the open sea. This assumption may be inadequate if the receiver is to be used in any environment in which there are objects that may block the LOS paths, which is often the case on land. Tools working under this assumption may predict that an acceptable number of satellites is visible, but in actuality some of those satellites may be hidden from the receiver by terrain or buildings.

As mentioned above, LOS obstructions may cause a GPS receiver to lose accuracy or even functionality. Receiver performance is especially an issue in mountainous or urban areas, commonly referred to as "urban canyons", where large portions of the sky can be blocked by buildings or terrain (Figure 5 below). Currently, there are no tools available that predict GPS satellite visibility while considering such LOS obstructions. This thesis presents *Satellite Viewsheds*: a new GIS tool that predicts GPS satellite visibility considering an area's features that may influence a receiver's performance. The tool can be used to predict performance for a receiver at any location on the earth's surface and for any time. The tool can also be used to determine the best time at which to use GPS for a given test day and location, and only requires a raster surface model grid and a text file describing the satellite's orbits. The new tool runs as a customization of widely available conventional GIS software and will allow a GPS user

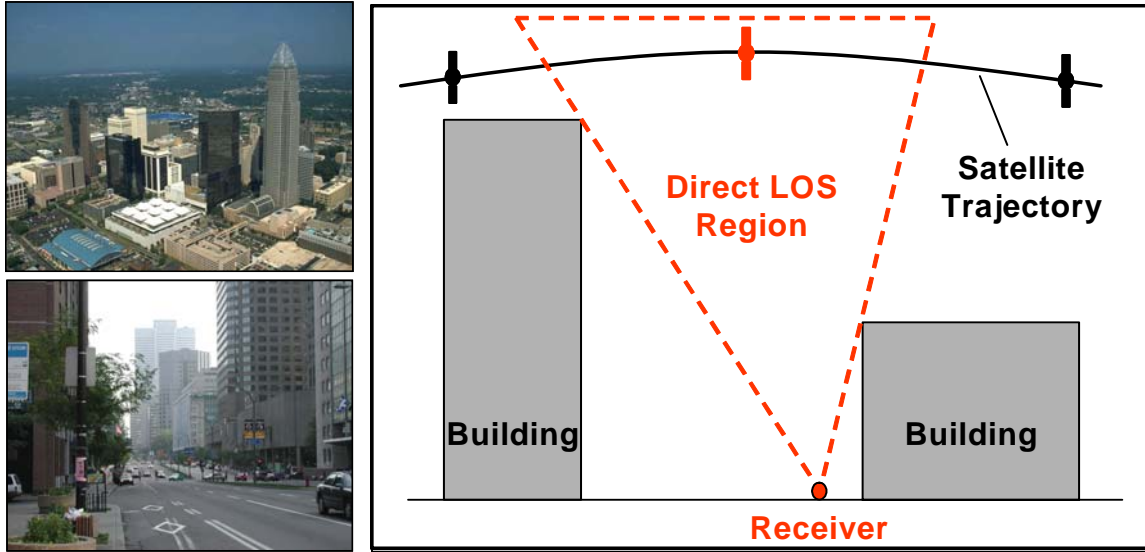


Figure 5. Examples of “urban canyons” in Charlotte, North Carolina (top left, photo credit: UNC Charlotte) and Montreal, Quebec (bottom left, photo credit: Jim Campbell), where large buildings can obstruct GPS signals and cause problematic reception. At right is a greatly simplified two-dimensional illustration of the urban canyon concept. Current satellite visibility tools predict reception from the satellite at positions 1, 2 and 3; but reception is actually possible only when the satellite is at position 2.

to determine: a) whether he or she will be able to use his or her receiver at all in a given area at a desired time, and b) if so, the time at which the maximum number of satellites will be visible during a specified day. The tool is easy to use, requires minimal user input, and is fully automated. Using the tool will allow GPS users, including researchers, surveyors, and sportspersons, to save time and money by pinpointing the time at which their receiver will produce the highest accuracy.

1.5 Fresnel Zones

Satellite Viewsheds performs its analyses with the assumption that if LOS cannot be established between a GPS receiver and a satellite, the receiver will not be able to use that satellite to triangulate its position. This means that the program does not consider the precise behavior of the radio signal transmitted by the satellite, such as reflection,

bending, or refraction. This assumption, which will be explained further in Chapter 3, is due primarily to the uniqueness of signal behavior to the specific environment in which it occurs. However, this paper does give consideration to one characteristic of telecommunications signals: Fresnel zones. A Fresnel zone is an area of secondary waves that encloses the direct LOS path in which a portion of a signal may be received (Baldassaro, 2001). The Fresnel zones considered in this research were used to analyze the knife-edge diffraction which occurs as a signal passes a sharp edge. As an example with a GPS signal, knife-edge diffraction may occur if a building corner is located near the direct LOS path between the receiver and a satellite. In this case, the receiver may still be able to acquire the satellite's signal even if the receiver is located just inside the building's shadow. The Fresnel zone effects considered in this research are discussed in Chapter 3.

Chapter 2. Project Justification and Literature Review

The preliminary literature research performed for this project was, in large part, focused on a search for existing tools that perform tasks similar to that of *Satellite Viewsheds*. The research also focused on the assessment of the need for *Satellite Viewsheds*. In addition, the research also included a literature review of selected previous studies that examined concepts relevant to this study, including the mathematics required for the calculation of the look angles.

2.1 GPS Reception in Difficult Areas

The signal reception loss that GPS users experience in mountainous or urban areas is well documented, and most regular GPS users have encountered problematic service at one time or another. In these areas, service may be lost completely or the accuracy of the position triangulation may be reduced. Figure 6 shows some online reviews of popular GPS receivers offered by Garmin, a well-known and respected GPS equipment provider. In a mountainous or urban area, if a GPS receiver does not cease operation due to its inability to acquire radio signals from a sufficient number of satellites, it may provide a highly erroneous position due to a concept called



Figure 6. Two online reviews of popular GPS units demonstrating the well-documented issue of signal loss in urban canyons, provided by www.epinions.com

multipathing. Multipathing occurs when the GPS receiver accepts signals that have been reflected before reaching the receiver (Figure 7). In some cases, the receiver may actually receive a signal from a satellite that it cannot see directly. Signal multipathing causes a problem for the receiver's position triangulation because the signal has traveled a longer distance than the actual distance between the receiver and the satellite. The extra distance adds extra time to the travel of the signal and the computation reflects this fact. Because the receiver uses the signal's time of travel to determine its distance from the satellite and hence its position, the receiver is "fooled" into thinking that it is somewhere other than its actual location. Signal multipathing is especially prevalent in urban areas, where the smooth glass and stone or concrete surfaces of buildings efficiently reflect signals without scattering them. Multipathing can also cause a GPS receiver to acquire two or more signals from the same satellite, which can confuse the receiver and produce a false reading (Kennedy, 1996).

GPS signal multipathing is almost impossible to predict because the varying conditions and features of local environments will cause signals to behave differently at each different location and at different times. Due to the difficulty in creating a universal

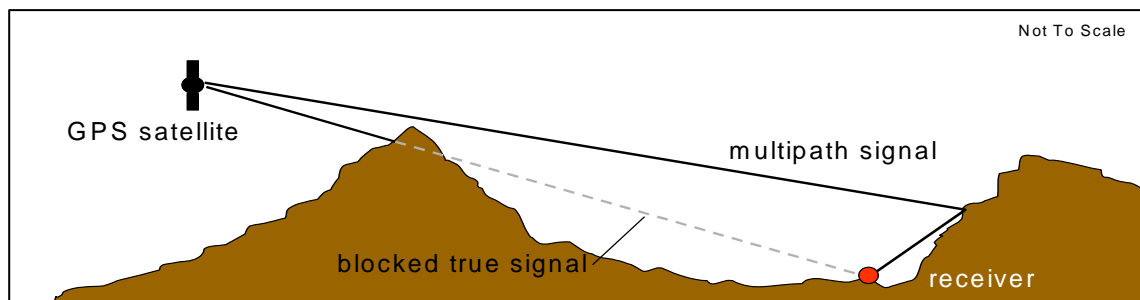


Figure 7. The concept of GPS signal multipathing. When the multipath signal reaches the receiver, it has traveled a longer distance than the actual distance between the receiver and the satellite.

multipath model, *Satellite Viewsheds* will perform its satellite visibility predictions based solely on the receiver's ability to establish direct LOS with the satellites. This assumption will be explained in further detail in Chapter 3.

The GPS industry is aware of poor reception in mountainous and urban areas, and there have been several technological innovations focused on providing accurate position information when GPS signals are lost. One such technology is Assisted GPS, or A-GPS. A-GPS is a general term describing a system in which outside sources, such as an assistance server and reference network, help a GPS receiver perform the tasks required to make range measurements and position solutions (LaMance et al, 2002). In order to make use of A-GPS, a standard GPS unit must be integrated with the proper equipment and must be used in an area in which local A-GPS networks are installed and in operation. Designed to assist emergency response personnel in locating a situation in need of attention, A-GPS provides many GPS service enhancements. One function of some A-GPS systems is to provide the receiver with its position when standard GPS reception is lost, allowing the unit to continue transmitting its position during an emergency. Typically, the A-GPS system uses special signals broadcasted from local cell phone towers to maintain positioning using its last known GPS position.

Another technological innovation focuses on reducing the effects of GPS signal loss in an on-board vehicle navigation system. The SBR-LS, produced by U-Blox, consists of a standard GPS navigation system that is designed to interface with two additional external sensors: a gyroscope to provide vehicle heading and an odometer

pulse to provide vehicle speed (U-Blox, 2001).

The navigation system uses information from these sensors to supplement the GPS positioning at all times. The primary benefit to the system is its ability to maintain the vehicle's position even when there is poor or no GPS reception. The SBR-LS was field tested in the urban canyons of New York, New

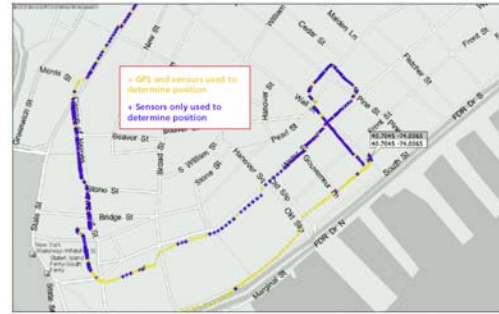


Figure 8. Results of the field test of SBR-LS in the urban canyon of Lower Manhattan. The yellow dots are data points collected by the sensor-based system activated after loss of GPS reception. Note the erroneous positioning due to multipathing of the signal (U-Blox, 2001).

York. Some of the results of the drive test are shown in Figure 8. The sensor-based system activated and maintained navigation when GPS reception was lost, but the figure shows the erroneous paths recorded due to the presence of the large buildings.

The technologies mentioned are just two examples of the ongoing research and development of GPS enhancement devices. However, as long as there are only 24 operational GPS satellites in orbit, a stand-alone GPS receiver will always experience problematic service in areas with LOS obstructions. In fact, it would take hundreds or even thousands of GPS satellites to alleviate all signal dead zones, which is obviously not feasible. Because full implementation of substitute service options such as those discussed above is not likely to occur in the near future due to their impracticality and expense, reception prediction is the only certain way to avoid areas and times of poor GPS receiver performance. The next section discusses the capabilities of current satellite visibility tools and the enhancements provided by the new ArcGIS tool.

2.2 Current Satellite Visibility Tools

There are many tools currently available that perform GPS satellite visibility prediction. Some may be included with a GPS package, others may be purchased separately, and still others may reside on the Internet as freeware. However, each of these tools falls short, in one way or another, of the objective of *Satellite Viewsheds*. Each existing tool researched performs a specific subtask of GPS satellite visibility prediction, and this research will show that the new tool pulls all of the subtasks together into one complete satellite visibility prediction program.

The first tool studied in the investigation of current software was the *Satellite Availability Program*, offered by Leica Geosystems. The tool is available online at no charge at www.leica-geosystems.com. *Satellite Availability Program* requires the observer's latitude and longitude, as well as an almanac file describing the orbits of the GPS satellites. Leica Geosystems' website provides almanac files updated daily for users to download. The program produces comprehensive charts and reports of GPS satellite visibility for a 24-hour period (Figure 9). *Satellite Availability Program* also allows the user the option of sketching or providing points for a model of the horizon surrounding the observer's point on a circular sky plot (Figure 10). Using this option does allow the user to incorporate local LOS obstructions into

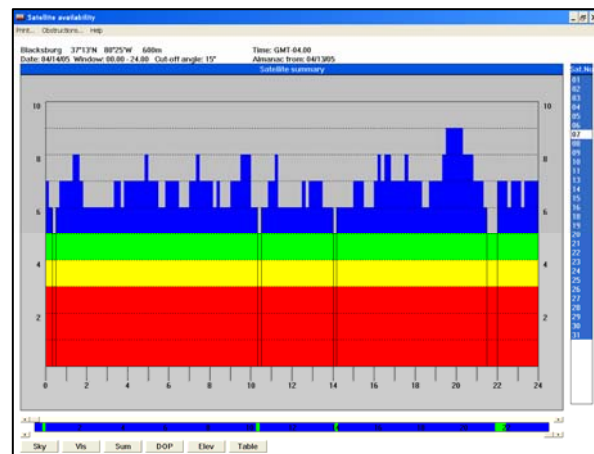


Figure 9. Example of GPS satellite visibility prediction using Leica's *Satellite Availability Program*, with time on the horizontal axis and number of satellites on the vertical axis

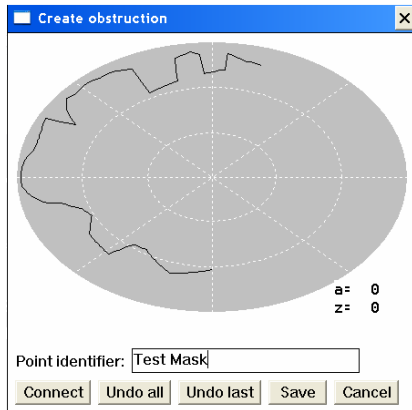


Figure 10. Example of a horizon mask input for the *Satellite Availability Program*

their GPS satellite visibility predictions, which is a primary objective of the new tool created for ArcGIS. However, in order to use the horizon masking option, a user must travel to the location at which he plans to use his GPS receiver and record the elevations and azimuths of all features on the local horizon before they run the visibility program.

For surveyors, this extra step may result in the expenditure of extra time and travel money while only improving the prediction at a single point.

While Leica Geosystems' *Satellite Availability Program* is a powerful and user-friendly GPS satellite visibility prediction tool, it does not address two important issues that are focal points of this research. As mentioned above, the only way to incorporate possible LOS obstructions in a GPS user's environment is to survey the horizon at the predicted point of data collection before the visibility tool is used. The new ArcGIS tool does not require the user to specify the characteristics of the local horizon. LOS obstructions exist in the surface model grid of the test area that the user supplies. No prior knowledge or surveying of the test environment is necessary before executing the program. The second restriction of the *Satellite Availability Program* that is addressed by the new tool is the fact that the predictions are performed only for a single point on the earth's surface. If a user desires to predict satellite visibility at multiple locations, which is almost always the case, then the program must be executed for as many times as the number of GPS points the user expects to collect. Additionally, if local LOS obstructions

were to be incorporated, the user would need to survey the horizon at all of the expected data collection locations before predicting satellite visibility. In the new ArcGIS tool, the visibility analysis is performed for an entire area in one execution. The user has complete control over the dimensions and location of the test area through their selection of the surface model grid.

A second GPS satellite availability software encountered during the background research was Trimble's *Planning Software*. This software is also available online free of charge at www.trimble.com. The program performs several satellite-related tasks, one of which is GPS satellite visibility from a user-specified location on the ground. User inputs for *Planning Software* include a test location, starting test date and time, number of time increments, time zone, and horizon masking angle. The tool produces reports and charts, such as the one shown in Figure 11, similar to those produced by Leica's *Satellite Availability Program*. While the user inputs to *Planning Software* are similar to those of the new ArcGIS tool, there is a major difference in the functions of the two tools. Like the *Satellite Availability Program*, incorporation of local LOS obstructions into satellite visibility predictions for the projected area of GPS receiver usage requires a preliminary

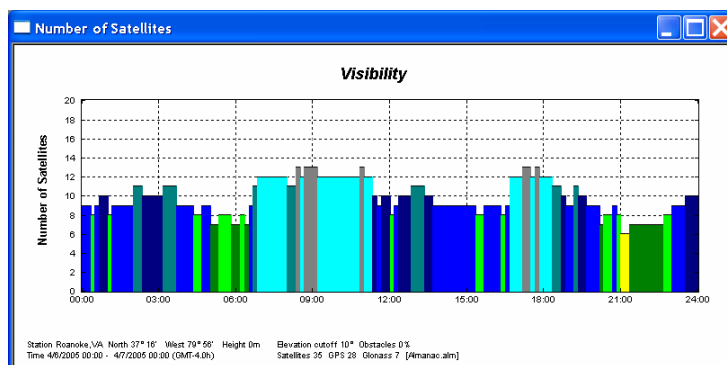


Figure 11. GPS satellite visibility predictions produced by Trimble's *Planning Software*

survey of the local horizon.

Also, the predictions can only be performed for one location per program execution.

Satellite Viewsheds addresses both of these issues by

alleviating the need for preliminary survey and performing visibility calculations across an entire area with one execution.

Another way for a GPS user to predict satellite visibility does not involve using computer software prior to data collection. Most newer GPS units include some type of satellite availability prediction tool within the units themselves. For example, the GPS receiver used for this project was Trimble's GeoXT unit, a member of the GeoExplorer Series. The unit includes Microsoft Windows Mobile 2003 software, which runs all operations available on the receiver. The program that operates the GPS antenna, TerraSync v.2.2 PE, allows users to record data points complete with feature attributes, either typed or voice recorded. The program also displays the current number of visible satellites on a circular sky plot and their azimuths and elevations, as well as the current Geometric and Position Dilutions of Precision (GDOP and PDOP, respectively), which will be discussed in Chapter 3. Another feature of the TerraSync software on the Trimble GeoXT is found under the "Plan" option and uses the most recent GPS almanac file it has received automatically to create a chart and sky plot providing the number of visible satellites continuously for the next one, two, three, four, six or 12 hours, as well as the look angles and PDOPs of the visible satellites (Figure 12). The user may also advance the timeframe to obtain satellite visibility



Figure 12. Trimble's *TerraSync* software on the GeoXT GPS receiver, predicting the PDOP and number of visible satellites for a 12-hour period

predictions for the next day and beyond. However, the TerraSync software presents similar restrictions to the objective of this project as those presented by the *Satellite Availability Program* and *Planning Software*. Even though TerraSync is on the GPS receiver, it cannot incorporate LOS obstructions at any time other than the present time of use. Without considering signal obstructions, the program may erroneously predict that certain satellites will be visible while in actuality, they will be hidden from the receiver by local surface features. In the simplified example of an urban canyon shown in Figure 5 (Chapter 1), a bare-earth prediction such as the one performed by TerraSync's Plan option will claim that the satellite will be visible at positions 1, 2 and 3. In reality, the satellite will only be visible to the receiver while it is at position 2. Additionally, the predictions are again performed only for one spot, the location of the unit at the time of analysis.

Research of GPS planning tools has shown that there is currently no efficient method of predicting satellite visibility for an entire area of interest while considering local LOS obstructions. *Satellite Viewsheds* performs visibility predictions for any area of the earth's surface at any time, as do the current tools. However, possible signal obstructions are also considered, a feature that is only offered for a single point with existing programs. The new tool provides a package of some features of existing tools while adding new, powerful capabilities afforded by the ArcGIS environment.

2.3 Justification

In addition to the literature research regarding current GPS satellite visibility tools, several GPS service providers were contacted with the intent of further investigating present capabilities of performing predictions using local terrain. The investigation confirmed the findings of the background research of current technologies, indicating that at this time, there is nothing available to perform the tasks addressed by the new ArcGIS tool. The research was performed through phone conversations with representatives of three GPS companies. The phone calls were not intended to be interviews, but rather conversations about the product lines of each company and their capabilities in satellite visibility prediction. During each phone call, the representative was asked if he knew of any tools, offered by his company or any other, that would assess satellite visibility across an entire area while considering local LOS obstructions. The conversations also included a short discussion on the benefits of such a tool. The three companies contacted were Garmin; DeLorme, a GPS, GIS and mapping software provider; and Earth Vector Systems, LLC, a provider of GIS, mapping, GPS and robotic systems for advanced surveying.

A software support representative from Garmin stated that the primary focus of their GPS software lies in mapping GPS data, not in mapping areas of weak signal reception. Any satellite visibility prediction capability that Garmin offers is built into the GPS receivers themselves, much like the TerraSync software discussed above (Garmin Sales Representative, personal communication, 2004). An analyst from DeLorme claimed that he did not know of any tools in the industry capable of predicting localized

satellite viewsheds. He said that the only way that he knew to incorporate terrain into visibility predictions was to survey the horizon of a test site before performing the prediction, as was the case with Leica's *Satellite Availability Program* and Trimble's *Planning Software* (DeLorme software support, personal communication, 2004). After listening to the objectives of the new ArcGIS tool, Bill Moore of Earth Vector Systems, LLD in Charlottesville, Virginia stated that there are bits and pieces available on the market that can perform each individual subtask. However, like the others, Mr. Moore did not know of any single tool that can perform all of the desired tasks and said that such a tool would need to be innovated (Moore, personal communication, 2004).

Each of the three GPS companies' representatives commented on the usefulness of a tool that can predict GPS receiver performance for a local environment. The general thought was that such a tool could save time and money for surveyors that intend to travel to a test time and that using the tool would ensure the most accurate data collection for a GPS user. In summarizing the research of existing GPS satellite visibility tools, there are many tools that perform predictions in one way or another. However, there are currently no tools that can predict GPS receiver performance for any area while considering local surface features that may partially or fully block GPS reception.

2.4 Relevance of Hillshades and Viewsheds

As discussed in Chapter 1, there are existing GIS surface analysis concepts that are relevant to the objective of the new tool: hillshades and viewsheds. ArcGIS offers functions that perform both of these operations on a valid raster surface model through

both its Spatial Analyst and 3-D Analyst extensions. To reiterate the objectives of *Satellite Viewsheds*, the tool must use multiple satellites (or view sources) that are located outside of the boundaries of the surface model grid to predict satellite visibility for a test area and time while considering local signal obstructions. The existing Hillshade and Viewshed functions each offer pieces of this objective, but neither fully performs the desired task

In ArcGIS, the Viewshed function requires an input surface grid and the location of the viewshed source point, points, area or areas. The viewshed algorithm then investigates each cell in the grid and determines whether or not the source(s) can be seen from that point. At every cell, the height or elevation of all cells between the current cell and the source is compared with the elevation of the line of sight at that location. If the terrain is higher than the line of sight at any point, then the cell under consideration is assigned a value of 0, meaning that the cell is hidden from view of the source. Again, viewsheds are typically used for applications such as optimizing forest fire tower locations for the largest possible viewsheds; or perhaps placing an unattractive feature at a low-visibility site. According to ArcGIS Desktop Help, the Viewshed function creates a raster recording the number of times each cell can be seen from the input point observer locations. Relating ArcGIS's Viewshed function to the goals of this research, there are several useful features that deserve mention. The Viewshed function does have the ability to handle more than one view source, and it does perform visibility analyses based on local LOS obstructions. However, one primary restriction of ArcGIS's Viewshed function prevents it from being used for GPS satellite visibility prediction. The routine is

only designed to handle view source points that are located within the boundaries of the surface model grid. This requirement is obviously insufficient for the accommodation of satellites that are thousands of kilometers from the test area. For this reason, the existing Viewshed function was not used in the creation of the new tool. However, the descriptive term “viewshed” will be used extensively throughout this paper because viewsheds are exactly what the new tool creates; one for each satellite at each test time.

Like the Viewshed function, ArcGIS’s Hillshade command requires an input surface grid, an azimuth and elevation for the imaginary light source, and whether or not to model shadows. As described in Chapter 1, hillshades are typically used to create 3-D visualizations of the terrain by shading the cells of the grid based on their illumination by the light source. The illumination is calculated based on the gradient and aspect of the cell. However, if the user chooses to “model shadows”, the Hillshade function essentially creates a viewshed using the light source as the view source by indicating those areas that are in a shadow from the light source. Areas that are hidden from the light source, perhaps behind buildings or mountains, are assigned a value of 0. The rest of the cells are assigned a value between 1 and 255, depending on their degree of illumination. The restriction of the Hillshade function that prevents it from being fully capable of predicting GPS satellite visibility is its inability to handle more than one view source. Therefore, the existing Hillshade function cannot be used as a stand-alone tool to perform the task at hand, which is to create viewsheds from multiple celestial sources.

2.5 Previous Works

The study of literature regarding this application of GIS to satellite visibility found no documented studies dedicated specifically to satellite viewsheds. The lack of published literature is perhaps due to the classified nature of satellite communications studies performed by the U.S. government and/or the relatively new capabilities of both GIS and satellite communications. However, there is an abundance of literature regarding studies of the behavior of wireless communication signals as well as GPS receiver accuracy. This section discusses several studies that are representative of the wealth of documented research on these topics.

GIS has been used to model signal source viewsheds many times and to determine the location of “dead zones”, or areas of little or no signal reception. In some cases, GIS capabilities for predicting signal reception has actually been studied. For example, a 1995 study by Cohen-Or analyzed GIS’s capabilities in the determination of viewsheds and the accuracy of signal-strength prediction using a DEM. GIS was used to predict dead zones and then those zones were field tested. For areas in which a signal was received contrary to the predictions of the GIS, a new visibility analysis was performed with higher resolution DEMs. The study determined that errors in that specific signal prediction were actually a result of the 30-meter resolution of the original DEMs being too coarse for the desired accuracy of the predictions. While this study considered cell phone signals instead of GPS signals and the signal sources were terrestrial, its implications are still useful to this project. The higher the resolution of the surface model, the more accurate the predictions of the new ArcGIS satellite viewsheds tool will

be. Therefore, a user of the new tool should provide a surface model that is of the highest resolution available. The study also indicated that GIS is capable of producing accurate signal reception models, given a surface model with sufficient resolution.

Research of previous works also discovered many studies that have been devoted to testing a GPS receiver's performance in a potentially problematic environment. For this project, studies such as these served to further document the loss of reception that may be experienced in urban canyons and thus reinforce the usefulness of the new ArcGIS tool. One study tested GPS receiver performance in the urban canyon of Calgary, Alberta (Melgard et al., 1994). The worst-case scenario recorded latitude readings in error of up to 40 m. The results of the test are shown in Figure 13.

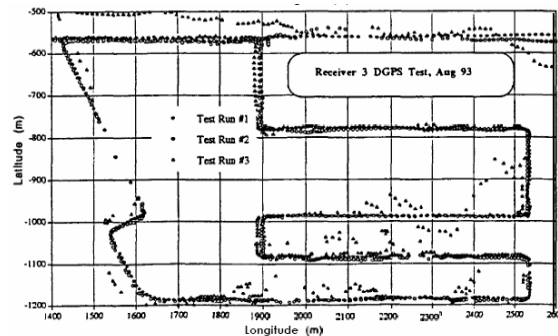


Figure 13. Three tests of GPS receiver performance at three different times, illustrating the inconsistent position data collection caused by the urban canyon of Calgary, Alberta (Melgard, et al.)

Another study of interest was actually performed at Virginia Tech and provided the background necessary to incorporate GPS signal behavior into this project. The study assessed the accuracy of wireless signal strength predictions using a GIS and the predictions were field tested. A surface model of the Virginia Tech campus was created through the appendage of a 30-m DEM in which building heights were added to the bare earth model. The model was similar to the 1-ft resolution campus model created for this project, which will be described in detail in Chapter 3. The study compared the actual

signal strengths with the predicted signal strengths for several different wavelengths. It was found that the larger wavelength signals (> 0.12 m) were more susceptible to multipath interference and were more apt to diffract around buildings and terrain features (Baldassaro, 2001). A GPS signal has a wavelength of 0.1904 m (Parkinson, 1996), greater than the threshold proposed by Baldassaro. Although the wavelength difference is relatively insignificant, the study reinforced the need to incorporate signal diffraction in any GPS satellite visibility predictions.

The Virginia Tech study incorporated knife-edge diffraction of the signals by calculating Fresnel zone widths. The Fresnel zone considerations in the study provided the basis for diffraction analysis in this project. The Fresnel zones considered in the Baldassaro study were based on the theory of knife-edge diffraction, shown in Figure 14. Knife-edge diffraction is a theoretical model of the diffraction that occurs when a sharp-edged object, such as the corner of a building, is located near a LOS path. Single knife-edge diffraction theory considers only one sharp edge and is the simplest and most understood type of diffraction (Baldassaro, 2001). The calculation of the width of the

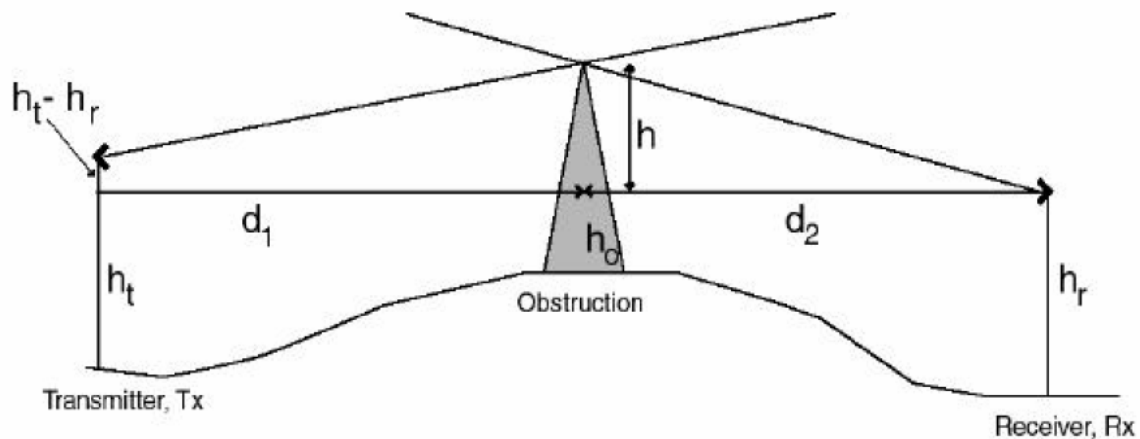


Figure 14. Illustration of single knife-edge geometry used in this research (after Baldassaro, 2001)

first Fresnel zone is a necessary step in determining the effect that single knife-edge diffraction can have on signal reception. The width of the first Fresnel zone (F_1) is an indicator of how close the “knife-edge” must be to the LOS path in order to affect the signal. The width of the first Fresnel zone for single knife-edge diffraction can be calculated using the following equation (Baldassaro, 2001):

$$F_1 = \sqrt{\frac{\lambda d_1 d_2}{(d_1 + d_2)}}; \quad \text{Eq. 2.1}$$

in which λ is the wavelength of the signal, d_1 is the distance from the transmitter (satellite) to the obstruction, and d_2 is the distance from the obstruction to the receiver. Equation 2.1 was used to calculate the widths of the first Fresnel zones associated with GPS signals and how they affect the results produced by the new satellite viewsheds tool. The results are discussed in detail in Chapter 3.

2.6 Look Angle Calculations

A major feature of the new ArcGIS satellite viewsheds tool is its ability to determine the locations of GPS satellites in the sky based solely on the time and surface location of interest. Most of the current tools described above in Section 2.2 require the user to provide an almanac file in order to calculate look angles. Almanac files can sometimes be downloaded online, but in many cases the user must acquire the file from an actual GPS unit prior to performing a visibility prediction. *Satellite Viewsheds* alleviates the need for an almanac file and only requires a user to download a pre-formatted TLES, which are readily available online. While the specifics of the programming algorithm will be discussed in Chapter 4, the mathematics used to calculate the look angle of a satellite are discussed in this section.

There are three pieces of data needed to calculate a satellite's position relative to a location on the earth's surface. The first requirement is the latitude and longitude of the terrestrial target. This information is extracted from the surface model grid provided by the user. The second piece of data is the orbital properties of the satellite, which are provided by the TLES. The third requirement for the calculation of a satellite's look angle is the exact time of interest, which is provided to *Satellite Viewsheds* by the user. Given these three pieces of information, it is possible to calculate where a satellite is in the sky relative to any point on the earth's surface. Before the discussion of the look angle calculations begin, it should also be noted that several assumptions are made in the calculations in this project. First, the orbits of the GPS satellites are assumed to be circular. Secondly, the location of the surface area is generalized to the location of the center point of the grid, meaning that satellites are at the same look angle from every cell in the grid. Also, the look angles are calculated under the assumption that the satellite and the earth are the only bodies influencing the satellite's trajectory, more commonly referred to as a "Two-Body Problem". In other words, the gravitational pull of the sun, the moon and other celestial bodies are not included in the calculations. These and other assumptions, as well as their benefits and potential for errors, are discussed in detail in Chapter 3.

All orbital properties of the satellite are drawn from the TLES file, input to the program in the form of a text (.txt) file. The mathematical properties of an orbit are called the "orbital elements". A full description of the TLES format and the information

they contain is provided in Chapter 3. In order to calculate look angles for a satellite in a circular orbit, the following pieces of information must be obtained from the TLES:

1. *Epoch Test Time*: the time at which the orbital elements were taken. The epoch test time is important because the orbital elements provided by the TLES change over time.
2. *Right Ascension of Ascending Node*, Ω : the longitude of the point at which the orbit crosses the equatorial plane moving south to north (Campbell, 2002)
3. *Argument of Perigee*, ω : the angle, in the plane of the satellite's orbit, between the ascending node and the orbit's closest point to the earth (point of periapsis), measured in the direction of the satellite's motion (Bate et al., 1971)
4. *Inclination*, i : the angle between the earth's polar axis and an orthogonal line to the satellite's orbital plane (Campbell, 2002)
5. *Mean Anomaly*, M_0 : position (in degrees) of satellite in orbit (for circular orbits, $M_0 =$ the true anomaly, v_0)
6. *Mean Motion*, n : the number of times, per day, that the satellite completes one revolution around the earth

Given these six values from the TLES, as well as a test time and location, the look angle can be calculated as shown below. For simplicity, only the primary steps will be included, omitting minor operations such as angle adjustments and unit conversions.

The first step in the look angle calculations is a simple but necessary one. The difference between the actual test time and the epoch test time (Δt) is determined, in the format 'days.fraction of day'. Also, the Local Sidereal Time (LST, Θ) at the time of test must be calculated. The LST is the angle between the local line of longitude and the

vernal equinox (Bate et al., 1971). The LST can be calculated from the Sidereal Time at Greenwich at a known time, or Θ_{g0} , which can be found in astronomical tables, usually for each year at midnight UTC on January 1. The LST is then calculated by (Bate et al., 1971):

$$\Theta = \Theta_{g0} + \omega_E(t - t_0); \quad \text{Eq. 2.2}$$

in which ω_E is the angular velocity of the earth, t is the test time and t_0 is the time of Θ_{g0} . Once these preliminary calculations have been performed, the geometry of the problem can be addressed. First, the semi-major axis of the orbit (a) is calculated. For circular orbits, the radius (r) is equal to the semi-major axis (Wertz et al., 1999):

$$a = \sqrt[3]{\frac{\mu}{n^2}}; \quad \text{Eq. 2.3}$$

in which μ is the earth's gravitational parameter. Next, the true anomaly at epoch is used to determine the true anomaly at test time (v) by adding the number of revolutions made by the satellite since the epoch to the true anomaly at epoch:

$$v = v_0 + n\Delta t \quad \text{Eq. 2.4}$$

Next, the components of the radius are determined in the perifocal frame (Wertz et al., 1999):

$$\mathbf{r}_p = [r \cos v; r \sin v; 0]^T; \quad \text{Eq. 2.5}$$

in which \mathbf{r}_p is the radius vector to the satellite in the perifocal frame. Then the position vector of the satellite must be rotated from the perifocal frame to the inertial frame. In order to perform the rotation, a transformation matrix (\mathbf{R}^{ip}) must be created (Wertz et al., 1999):

$$\mathbf{R}^{ip} = \begin{bmatrix} \cos \Omega \cos \omega - \sin \Omega \sin \omega \cos i & -\cos \Omega \sin \omega - \sin \Omega \cos \omega \cos i & \sin \Omega \sin i \\ \sin \Omega \cos \omega + \cos \Omega \sin \omega \cos i & -\sin \Omega \sin \omega + \cos \Omega \cos \omega \cos i & -\cos \Omega \sin i \\ \sin \omega \sin i & \cos \omega \sin i & \cos i \end{bmatrix}$$

Eq. 2.6

To complete the rotation, the satellite's position vector in the perifocal frame is multiplied by the transformation matrix to obtain the position vector in the inertial frame (Wertz et al., 1999):

$$\mathbf{r}_i = \mathbf{R}^{ip} \mathbf{r}_p = [r_1; r_2; r_3]$$

Eq. 2.7

From the position vector in the inertial frame, the sub-satellite point (latitude $[\delta_s]$ and longitude $[L_s]$ of the earth's surface directly beneath the satellite) can be determined (Wertz et al., 1999):

$$\delta_s = \sin^{-1} \left(\frac{r_3}{r} \right)$$

Eq. 2.8

and:

$$L_s = \tan^{-1} \left(\frac{r_1}{r_2} \right) - \theta_{g0}$$

Eq. 2.9

Now that the location of the sub-satellite point is known, the look angles can be determined.

Using the earth-satellite geometry shown in Figure 15 below, the elevation and azimuth angles can be calculated. First, the Earth angular radius (ρ) is calculated (Wertz et al., 1999):

$$\sin \rho = R_E / r;$$

Eq. 2.10

in which R_E is the radius of the earth. The Earth central angle (λ) can also be calculated (Wertz et al., 1999):

$$\cos \lambda = \cos \delta_s \cos \delta_t \cos \Delta L + \sin \delta_s \sin \delta_t; \quad \text{Eq. 2.11}$$

in which δ_t is the latitude of the test point and ΔL is the longitude difference between the sub-satellite point and the test point. Next, the nadir angle (η) can be calculated (Wertz et al., 1999):

$$\tan \eta = \frac{\sin \rho \sin \lambda}{1 - \sin \rho \cos \lambda} \quad \text{Eq. 2.12}$$

Finally, the elevation angle (ε) and the azimuth angle (Az) of the satellite can be calculated (Wertz et al., 1999):

$$\varepsilon = 90^\circ - \eta - \lambda \quad \text{Eq. 2.13}$$

and:
$$\cos \text{Az} = \frac{\sin \delta_t - \cos \lambda \sin \delta_s}{\sin \lambda \cos \delta_s} \quad \text{Eq. 2.14}$$

In *Satellite Viewsheds* for ArcGIS, the program performs these calculations automatically for each GPS satellite provided by the TLES, at every test time specified by the user.

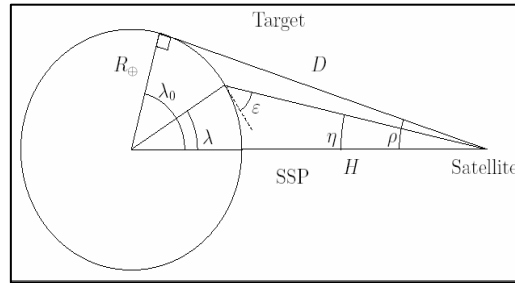


Figure 15. Target-satellite geometry (Wertz et al., 1999)

2.7 Literature Review Summary

There is an abundance of literature regarding GIS viewsheds, problematic GPS reception in urban areas, signal behavior such as Fresnel zones and satellite look angle calculations. However, there were no previous works or tools found that combine all of these concepts. Considering the immense reliance of millions of people worldwide on

GPS, the fact that no one has created a comprehensive satellite prediction tool is somewhat surprising. This project will provide a major step towards achieving that task. The background research has shown that the new *Satellite Viewsheds* will be the first of its kind.

Chapter 3. Data and Assumptions

This chapter will discuss the purpose and format of data that *Satellite Viewsheds* requires as input; the data used for testing the accuracy of the new tool and how it was derived; and the assumptions made throughout the project.

3.1 Two-Line Element Sets Described

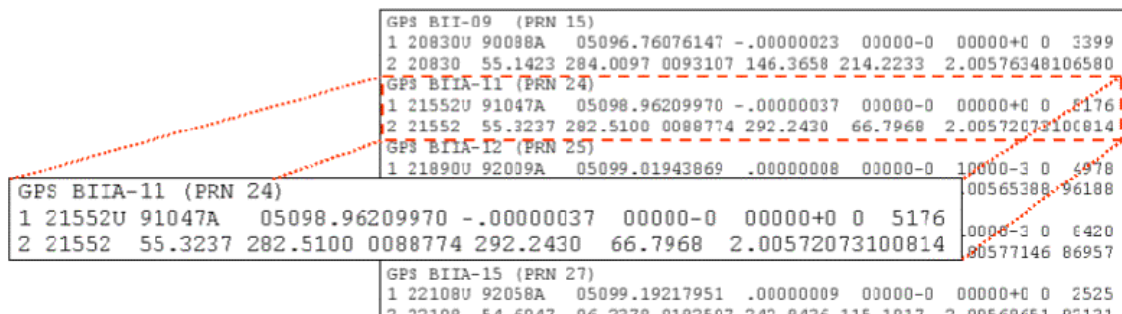
The discussion of required data for the program begins with perhaps the most fundamental element: the Two-Line Element Set describing the satellites' orbits. TLES was chosen as the format by which the program will receive orbital properties because of their standard, consistent format and their widespread availability. TLESs can be downloaded online in a matter of seconds. At the time of this paper's writing, the recommended site for acquiring TLESs is

www.celestrak.com, a well-known and respected source for data pertaining to public satellites. The site offers element sets for many satellites (Figure 16), including GPS, and the sets are provided as text (.txt) files. Because the satellite viewsheds tool requires the sets in .txt files, the user does not need to open or edit the sets; they can be simply downloaded and saved. CelesTrak updates their element daily, obtaining the data from the North American Aerospace Defense Command (NORAD)

Special-Interest Satellites		
Last 30 Days' Launches		
International Space Station		
100 (or so) Brightest		
Weather & Earth Resources Satellites		
Weather		
NOAA		GOES
Earth Resources		
Search & Rescue (SARSAT)		Disaster Monitoring
Tracking and Data Relay Satellite System (TDRSS)		
Communications Satellites		
Geostationary		
Intelsat		
Gorizont	Raduga	Molniya
Iridium	Orbcomm	Globalstar
Amateur Radio	Experimental	Other
Navigation Satellites		
GPS Operational		Glonass Operational
Navy Navigation Satellite System (NNSS)		
Russian LEO Navigation		
Scientific Satellites		
Space & Earth Science		
Geodetic		Engineering
Education		
Miscellaneous Satellites		
Miscellaneous Military		Radar Calibration
CubeSats		Other

Figure 16. Two-Line Element Sets provided by CelesTrak.com

in Colorado Springs, Colorado. The sets contain three lines of data for each satellite, and one file lists the three-line sets for all satellites in a constellation consecutively (Figure 17). For a given satellite, Line 0 (the top line) contains the name of the satellite and/or an identifier. A sample title line for a GPS element set is “GPS BIIA-11 (PRN 24)”. Because this GPS satellite is usually more identifiable to the public as only “PRN 24” or “24”, *Satellite Viewsheds* extracts the parenthesized information and discards the rest.



GPS BII-09 (PRN 15)												
1	20830U	90088A	05096.76076147	-.00000023	00000-0	00000+0	0	3399				
2	20830	55.1423	284.0097	0093107	146.3658	214.2233	2.00576348106580					
GPS BIIA-11 (PRN 24)												
1	21552U	91047A	05098.96209970	-.00000037	00000-0	00000+0	0	5176				
2	21552	55.3237	282.5100	0088774	292.2430	66.7968	2.00572073100814					
GPS BIIA-12 (PRN 25)												
1	21890U	92039A	05099.01943869	.00000008	00000-0	10000-3	0	4978				
								00565388				96188
GPS BIIA-11 (PRN 24)												
1	21552U	91047A	05098.96209970	-.00000037	00000-0	00000+0	0	5176				
2	21552	55.3237	282.5100	0088774	292.2430	66.7968	2.00572073100814					
								00000-3				0420
								00577146				86957
GPS BIIA-15 (PRN 27)												
1	22108U	92058A	05099.19217951	.00000009	00000-0	00000+0	0	2525				
2	22108	54.6047	06.2278	0192597	242.8426	115.1817	2.00568651					07121

Figure 17. Partial GPS TLES with the elements for the single satellite PRN 24 inset

Lines 1 and 2 contain identifying information, values used to predict the movement and orbit of the satellite, and the time at which the values were taken. Below, Table 1 describes the information contained in a sample TLES that *Satellite Viewsheds* accepts. For an explanation of all items in a TLES, please refer to ‘Documentation’ at www.celestrak.com. The format shown below is the standard and all element sets produced should match this format. The gray dots in between items were added to allow for column number indexing. The following is a sample Line 1 and Line 2 from a GPS satellite element set, accompanied by a table describing the items. The red items are the values extracted by *Satellite Viewsheds*:

1 · 21552U · 91047A · - - 05098.96209970 - - .000000037 - - 00000-0 - - 00000+0 · 0 - - 5176
 2 · 21552 · - 55.3237 · 282.5100 · 0088774 · 292.2430 · - 66.7968 · - 2.00572073 100814

Field	Column	Item	Sample Value	Units
1.1	1	Line Number of Element Data	1	
1.7	19-20	Epoch Year (last 2 digits)	05	years
1.8	21-32	Epoch (day of year and fractional portion of day)	098.96209970	days
2.1	1	Line Number of Element Data	2	
2.3	9-16	Inclination	55.3237	degrees
2.4	18-25	Right Ascension of the Ascending Node	282.5100	degrees
2.6	35-42	Argument of Perigee	292.2430	degrees
2.7	44-51	Mean Anomaly	66.7968	degrees
2.8	53-63	Mean Motion	2.00572073	revs/day

Table 1. TLES format and description of items (Kelso, 2004)

The items presented by the TLES that are not used by the satellite viewsheds program include satellite classification and launch information, a drag indicator, and values that would be required for a higher level orbit determination than the one performed by *Satellite Viewsheds*. For higher accuracy, it is recommended that the user obtain a TLES that is as close to the test date as possible. While even one-month old element sets will usually cause relatively small errors in the look angle calculations ($<1^\circ$, Table 2), these errors can be avoided by downloading the most current data. The table shows look angle predictions by the new tool

using a TLES that is six weeks old compared with WinOrbit's most accurate calculations using a TLES published the day of the test. While some of the calculations using the old

Satellite	WinOrbit (e>0, drag, SG4)		Program (Old TLES)	
	Az (deg)	EI (deg)	Az (deg)	EI (deg)
PRN 03	309	27	309.8	26.4
PRN 06	167	18	166.1	18.8
PRN 15	295	55	295.2	56
PRN 16	258	14	257.3	14.7
PRN 18	239	73	235	74
PRN 21	89	76	87.7	74.6
PRN 22	239	40	236.8	39.8
PRN 26	67	43	68.3	43.4
PRN 29	51	32	51.2	32

Table 2. Comparison of look angle calculations performed with current and six-week old Two-Line Element Sets

TLES are within a degree of the actual values, other angles are in error by as much as 4°, such as the azimuth for satellite PRN 18.

3.2 User-Inputs

In continuing with the discussion of the user-provided aspect of the data for this project, this section describes all of the required user inputs to *Satellite Viewsheds* for ArcGIS except for the previously discussed element sets. Figure 18 shows the user form

Satellite Viewsheds

Input Files

i Surface model grid: No grid selected ...

Two-line element set file: No TLES file ...

c Minimum elevation angle (deg): 10

m **Z Factor of Surface Model**

☐ Enter manually

☒ Calculate based on coordinate system

Z units of surface model: Meters

j **Test Date**

February 17 2005

l **Time Zone of Test Site**

Eastern ☐ Daylight ☒ Standard

k **Time of Test (Local Time Zone)**

☐ Single test time

☒ Time range

Initial test time: 12 21 PM

Ending test time: 10 55 PM

Number of tests: 8

a ☒ Create program summary report

Name (no ext.): Summary

d Name of folder into which output grid(s) will be saved: TimeRangeGrids
(If folder exists, it will be overwritten.)

h Quit **b** Help **f** Reset **g** Run

e Program progress...

Figure 18. User interface for *Satellite Viewsheds* in ArcMap

that displays when *Satellite Viewsheds* is selected in the ArcMap window, and each letter corresponds to the item's description below:

a) *Create program summary report:* The program summary report provides details of the test, including the time, date, time zone, z factor (see item (m) below) and the look angle and percent coverage for each satellite at each test time. The report is saved as a text (.txt) file in the working directory, if the user opts to create one. If a report with the same name and path as the one specified by the user already exists, it will be overwritten. The default name for the report file is "Summary", but the user can specify any name with valid characters (a-z, 0-9).

b) *Help button:* Clicking this button will display a user form, with additional information about each user input.

c) *Minimum elevation angle:* Satellites at elevation angles below this value, measured in degrees will not be considered to be visible. The standard horizon masking angle is 10 degrees, and the value entered is required by the program to be between 0 and 90. Signals transmitted by satellites at low elevation angles are more susceptible to atmospheric disturbance because they travel a longer distance through the earth's atmosphere.

d) *Name of folder into which output grid(s) will be stored:* The user has the option to specify the name of a folder into which the output grid(s) will be saved, in the working directory. If a folder with that name already exists, it will be overwritten, so the user should use caution. For a single test time, the default folder name is 'SingleTestTimeGrid' and the default for a test time range is 'TimeRangeGrids'.

e) *Program Progress:* A progress bar that automatically updates after the 'Run' button has been clicked. While the speed of the program varies with computer speed, surface model grid size, number of satellites in the TLES and the number of test times, the user

should allow at least ten minutes of running time for a full GPS constellation and the maximum number of test times.

f) *Reset button*: Clicking this button resets all form values to initial values. The initial values for the time and date options are the current time and date.

g) *Run button*: The user clicks this button when he or she has completed data entry on the main user form. The button executes the program itself.

h) *Quit button*: Clicking this button exits the program and returns the user to the ArcMap window.

i) *Surface model grid*: The dialog box will prompt the user to select the auxiliary (.aux) file that represents the DEM, LiDAR or other surface model grid on which the viewsheds will be performed. The user must ensure that the .aux file selected is a component of a valid Raster Dataset. The directory in which the selected grid resides will become the working directory for the program, into which the report and the output grid(s) will be saved. If for some reason, the program cannot determine the coordinate system of the grid, the user will be prompted to provide the latitude and longitude of the center of the grid, in decimal degrees. To do this, the user should change the display units of the ArcMap data frame to 'Decimal Degrees' and hover the cursor over the center of the grid.

j) *Test date*: The date on which the satellite visibility analysis is to be performed, in the local time zone of the test site. If the user desires to perform the predictions for a range of times, the test date specified must be the date of the *first* test time.

k) *Time of test*: The user selects whether to perform the satellite visibility analysis for a single time or across a range of times. The time(s) specified must be in the time zone of the test site. For the single test time option, one grid is created depicting the number of satellites visible at the specified time. For the time range option, two grids are created: one grid containing the maximum number of satellites visible at any of the test times

across the time range and one grid depicting the time at which the maximum satellites are visible. These two grids may be combined after the program has finished by entering 'combine([MaxVisSats], [BestTime])' into the Raster Calculator. This will create a grid with unique classes based on both the best viewing time and the number of satellites visible at that time. Note: for the time range option, if a cell has the same maximum number of satellites visible at multiple, but not all, test times, the BestTime grid created will show that cell as having its maximum visibility time at the first time at which the maximum number of satellites is visible, by default.

l) *Time zone of test site*: The user specifies the time zone in which the surface model grid is located. The default time zone is 'Eastern', but any time zone in the world can be specified. On the initial user form, the user may select 'Eastern', 'Central', 'Mountain', 'Pacific', or 'Other'. If 'Other' is selected, a new user form displays allowing the user to select any time zone in the world, from Greenwich Mean Time (GMT) –12 to GMT +12. The time zone is used to rectify the test time(s) with GMT, which is the time zone of the satellite orbit data in the TLES.

m) *Z factor*: The z factor quantifies the relationship between the horizontal and vertical units of the surface model grid. For example, if the horizontal units are meters and the vertical units are in feet, the z factor is 0.3048. It is recommended that the user specify the vertical units and allow the program to calculate the z factor automatically. The program can calculate the z factor for vertical units of feet or meters. If the elevation values of the surface model grid are not in feet or meters, the user should enter the z factor manually. Also, the program can automatically calculate the z factor for surface model grids with the following coordinate systems: Universal Transverse Mercator (UTM); State Plane Coordinate System (SPC); and Geographic (lat/long). Table 3 shows the z factors for all scenarios automatically accommodated by the tool:

If the program encounters difficulty in its automatic determination of the coordinate system, the user is prompted to provide a z factor. To manually calculate a z factor, the problem can be thought of as "How many horizontal units are in one vertical unit?"

Coordinate System of Surface Grid	Horizontal Units	Vertical Units	Z Factor
Geographic	Decimal Degrees	Feet	$8.983e-6 / \cos(\text{latitude})$
Geographic	Decimal Degrees	Meters	$2.738e-6 / \cos(\text{latitude})$
State Plane (SPC)	Feet	Feet	1
State Plane (SPC)	Feet	Meters	3.2808
Universal Transverse Mercator (UTM)	Meters	Feet	0.3048
Universal Transverse Mercator (UTM)	Meters	Meters	1

Table 3. Z factor calculations for all coordinate systems and vertical units accommodated by the program

3.3 Virginia Tech Campus Test Data

To verify the results of the new satellite viewsheds program, its results were tested on the Virginia Tech campus in Blacksburg, Virginia. In order to test the area, a surface model grid of the campus, including buildings, was needed. Raster models of the Virginia Tech campus have been created in the past, including the ones shown in Figure 19. The grids, used in the study by Baldassaro (2001), consist of campus building footprints with heights laid on top of a DEM of the area. The full process by which the grids were created is outlined in Rose (2001). Due to the grids' creation dates, however, some newly constructed buildings are not included. Also, the old grids do not include ridges on roofs of buildings which can obstruct a signal. In addition, a model with a slightly higher resolution than the 1-meter resolution of Rose's grid (Figure 19) was desired for testing of the new ArcGIS tool. Therefore, it was necessary to create a new surface model of campus that included the features not present in the old grids.

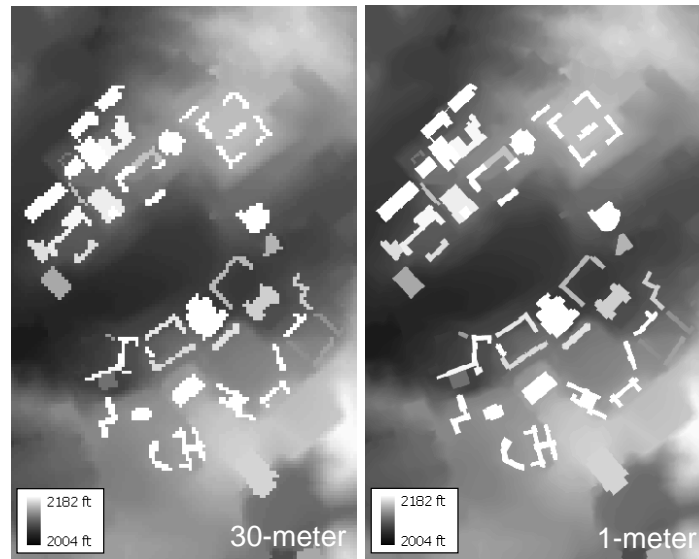


Figure 19. Appended 1- and 30-meter DEMs of the Virginia Tech campus used in previous studies by Rose (2002) and Baldassaro (2001)

The first step in the creation of the new surface model grid of Virginia Tech was to obtain all data required by the process. Virginia Tech's Capital Design and Construction Department (CDCD) provided polyline shapefiles containing 1-foot bare-earth elevation contours, building roof outlines and roof ridges, and spot elevations across campus, as shown in Figure 20 below. From the contours and building outlines, a Triangular Irregular Network (TIN) was created through the ArcGIS 3D Analyst extension (Figure 21). A TIN is a network of triangular facets with their vertices at the known locations of the points and lines provided by the users. TINs reflect changes in continuous data such as elevation. After the TIN depicting the bare-earth elevation of campus was created, it was converted to raster grid format with a cell size of 1 foot, using the 3D Analyst option 'TIN to Raster' (Figure 22). Next, a new polygon shapefile was created, and each of the outlines of the buildings in the polyline shapefile was digitized, creating a polygon for each campus building. Because the building outline polyline file received from CDCD included an elevation attributed, each building polygon was

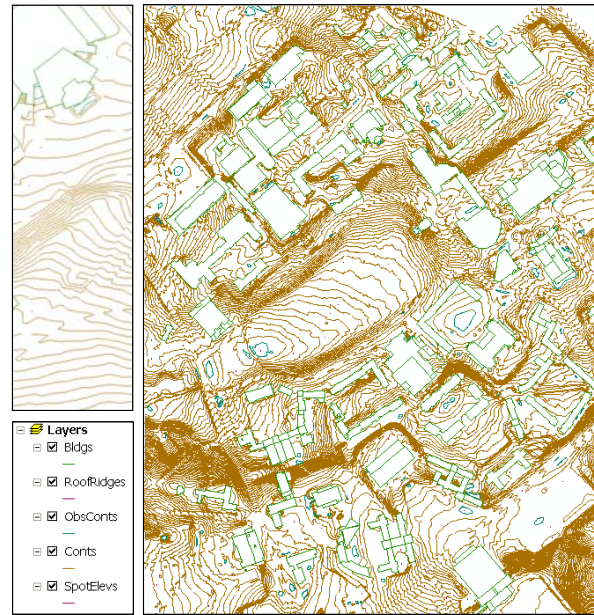


Figure 20. Vector data of the Virginia Tech campus including elevation data; obtained from CDCD

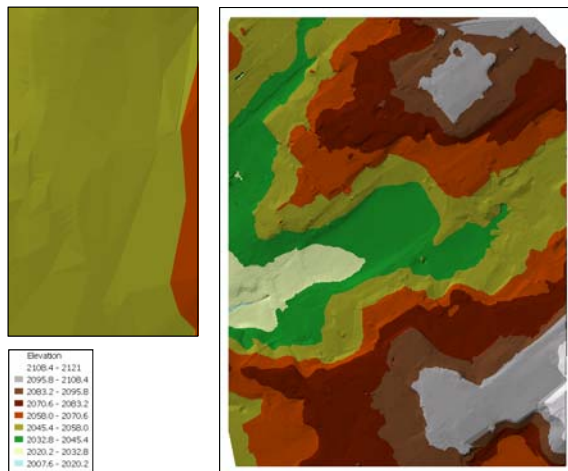


Figure 21. TIN of the 1-foot elevation contours of the Virginia Tech campus

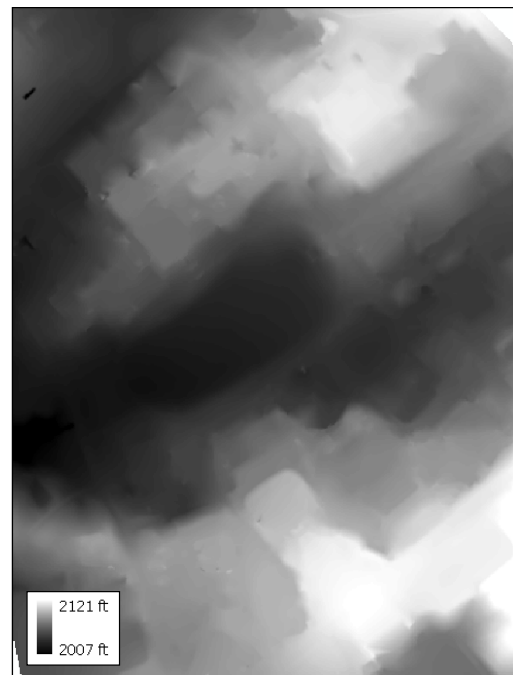


Figure 22. Bare-earth elevation grid of the Virginia Tech campus created from the TIN shown in Figure 21

assigned the elevation of the polylines from which it was digitized. Next, the roof ridges were digitized into the building polygon file with their elevation attributes. For simplicity, on triangular-shaped roofs, the apexes of the roofs were digitized as long, slender polygons because they cast effectively the same shadows as triangular roofs of the same height. Once the building polygons were complete with roof features, they were converted to raster through the ArcGIS Spatial Analyst extension. Finally, the raster buildings were overlaid with the bare-earth elevation model, creating the 1-foot resolution grid shown in Figure 23. The grid measures 0.55 by 0.70 miles, or 2889 by 3679 pixels.

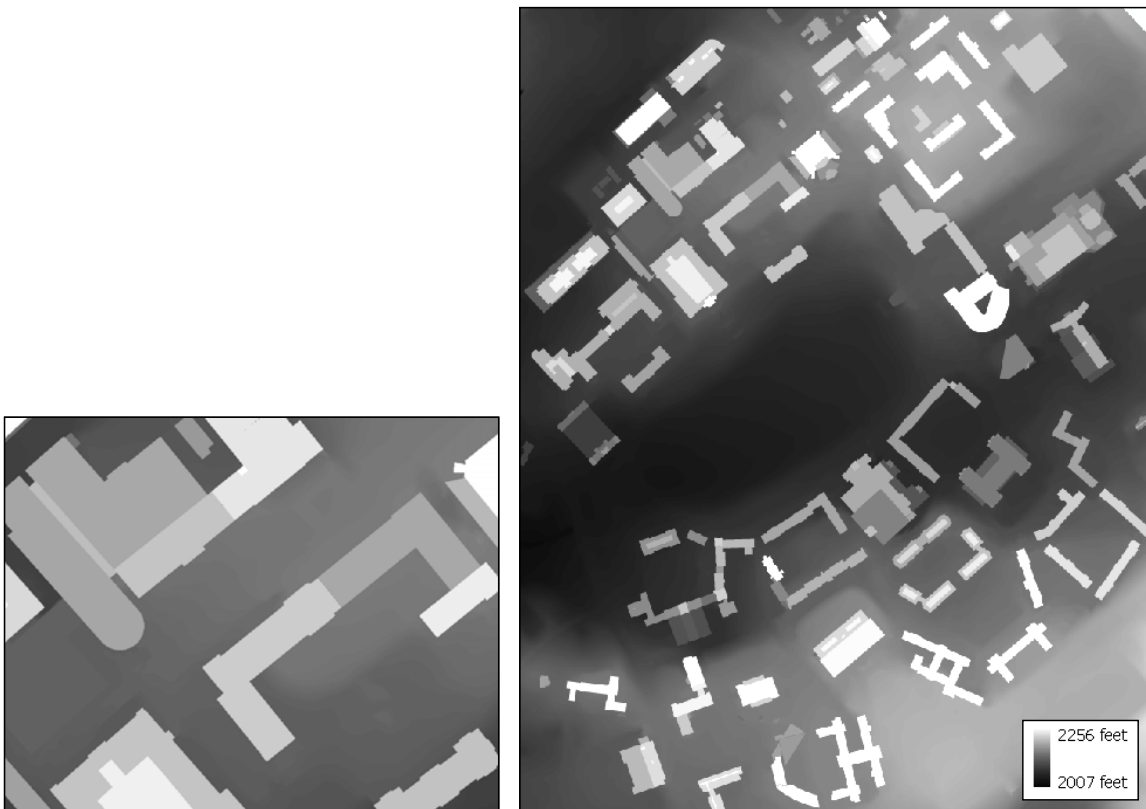


Figure 23. 1-foot surface model grid of the Virginia Tech campus used to test the satellite viewsheds tool. A close-up view is shown in the inset.

3.4 Assumptions

Several assumptions were made during the creation of *Satellite Viewsheds*. The simplifications will be discussed in this section. In addition, the effects of the mathematical assumptions on the accuracy of the relevant calculations in the worst-case scenarios are provided. The majority of the assumptions made regarded the look angle calculations of the satellites. The assumptions were made for simplicity; based on the fact that the creation of a full, working GIS program was the primary focus of the project. Unfortunately, time did not permit the application of higher-level astrodynamics in the look angle calculations. However, field testing will show that the calculations performed by the new tool are sufficient and comparable to more complex higher-level calculations.

3.4.1 Two-Body Systems

The first assumption made during the look angle calculations was that the earth-satellite relationship is a two-body problem. In a two-body problem, all gravitational effects of other celestial bodies, such as the sun and the moon, are not considered. Also, the earth was assumed to be either a point in space with the earth's mass, or equally, a perfect sphere with uniform mass distribution. In reality, the earth is oblate, with bulges and dips in the surface, and the polar axis is about 0.33% shorter than the equatorial axis (Carstensen, 2003). Modeling the satellite-earth relationship as a two-body problem means that all orbital elements, except for the true anomaly, are constant throughout a satellite's orbit. In addition, the mass distribution throughout the interior of the earth is not uniform with some areas being denser than others. Because gravitational force is caused by a collection of mass, the non-uniform mass distribution throughout the earth

and the planet's slightly irregular shape create a non-uniform gravitational field. A satellite orbiting the earth at a constant altitude will experience varying gravitational attraction from the earth, altering the dynamics of the satellite's movement. Other variables that could possibly affect a satellite's orbit that were ignored included atmospheric drag and solar radiation pressure.

3.4.2 Circular Satellite Orbits

The final assumption regarding the look angle calculations was that GPS satellites are in circular orbits, allowing for simpler mathematics in the determination of the look angle. In reality, GPS satellite orbits are slightly elliptical with flattening (eccentricity) ranging from just greater than 0 to around 1/50 (2%), with most having eccentricities of less than 1%. The effect that each individual assumption had on the look angle calculations was not examined, but their collective impact was assessed through the look angle verifications discussed in Chapter 5.

3.4.3 Flat Earth Study Area

Other assumptions made by *Satellite Viewsheds* may also affect the look angle calculations. First, the earth's curvature across the test area is ignored. For optimal results, the satellite viewsheds tool is designed for large scale, small area test sites, such as several city blocks. For example, the surface model grid of the Virginia Tech campus created for this project measures 0.55 by 0.70 miles. Even for relatively large test areas that may be tens of miles across, the earth's curvature is negligible, and any curvature that exists is likely to be voided by local terrain features.

3.4.4 Satellite Position

Also, a given satellite is assumed to be in the same position relative to every cell in the grid. Because of the immense distance between GPS satellites and a target location on the earth's surface, the difference between the look angles to a satellite for different cells in the grid is very small. As an example, Table 4 shows the differences in satellite elevation angles between two cells that are 1 and 10 miles apart. The calculations were performed using an average satellite-to-target distance (range) of 14,000 miles. The table shows that using the same look angle for all cells in the test are creates only a negligible error for even large grids covering a 10-mile region.

Cell Separation (mi)	EI 1 (deg)	EI 2 (deg)	Diff (deg)
1	15	14.9989	0.0011
1	30	29.9987	0.0013
1	60	59.9965	0.0035
10	15	14.9894	0.0106
10	30	29.9803	0.0197
10	60	59.9646	0.0354

Table 4. Comparison of satellite elevation angles from cells spaced 10 miles apart

3.4.5 Sea Level Assumption

The final assumption involving the satellite look angles sets the elevation of the entire test area to 0 during the calculations, due to the varied elevations across an area and the non-spherical surface of the earth. Table 5 shows the differences in predicted satellite elevation angles between a spherical sea level and an observer at an elevation of 10,000 feet, again for a target-satellite range of 14,000 miles.

Elevation 1 (ft)	Elevation 2 (ft)	EI 1 (deg)	EI 2 (deg)	Diff (deg)
0	10,000	15	14.9920	0.0080
0	10,000	30	29.9936	0.0064
0	10,000	60	59.9952	0.0048

Table 5. Comparison of satellite elevation angles from a target at an altitude of 0 and another at an altitude of 10,000 ft

3.4.6 Assumption of Complete GPS Constellation

The program assumes that all the satellites listed in the input TLES are in operation and transmitting. However, the element sets provided by NORAD include spare satellites that provide backup for any operational satellites that might experience problems. There are 24 operational GPS satellites, but NORAD's element sets often list 29. Because GPS satellites are interchanged as needed, it is up to the user to determine which satellites are spares and remove them from the TLES before running *Satellite Viewsheds*.

3.4.7 A Final Issue of Note

If the user chooses to perform a satellite visibility prediction for a range of times, the program produces two grids: one showing the maximum number of satellites visible from each cell at any of the test times; and another showing the time at which the maximum number of satellites are visible (Figure 24), called the "Best Time" grid. The

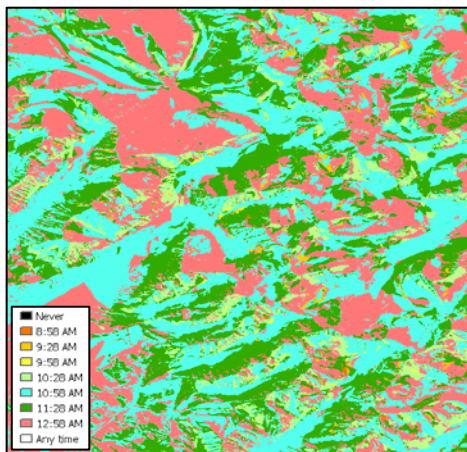


Figure 24. Sample output grid for the GIS tool's time range option. The map shows the time at which the maximum number of satellites is visible from each pixel

grid displays the test time at which the most satellites are visible, but this time is not necessarily the time at which the GPS receiver will provide the highest accuracy. While the number of visible satellites is a reliable indicator of receiver accuracy, the PDOP is the most important factor in a receiver's performance.

PDOP is calculated based on the geometry of the visible satellites and the target location, and

provides a measure of the extent to which satellite geometry exacerbates other errors that may occur in the measurements (Kennedy, 1996). The triangulation routine performed by the receiver in its position calculation is most accurate when the satellites are the furthest apart from one another in the sky. The absolute optimal positioning for four GPS satellites relative to a ground target is one satellite positioned directly overhead and the three others positioned near the horizon, spaced evenly in a circle at intervals of 120° (Kennedy, 1996). Perfectly positioned satellites produce a PDOP value of “1”, and as the value increases, positional accuracy decreases. On most GPS units, the maximum PDOP value at which positions will be recorded can be specified by the user; but the default value is usually 6.0.

PDOP is mentioned here because there may be cases in which the maximum number of visible satellites for a receiver does not guarantee the most accurate positioning. For example, if there is one test time in which there are six satellites visible and another time at which seven satellites are visible, the accuracy of the position triangulation may be slightly higher at the time of six visible satellites due to a better satellite-target geometry. *Satellite Viewsheds* does not calculate PDOP, but the situation in which the time of the best PDOP value does not match the time of maximum visible satellites is rare. To illustrate this point, Leica’s *Satellite Availability Program* was used to create the graph shown in Figure 25. The visibility predictions were performed for Blacksburg, Virginia, using all GPS satellites (including spares) for a 24-hour period. The gray shaded areas represent the number of visible satellites and the red line indicates the PDOP. The graph clearly shows the high correlation between the times of maximum

satellite visibility and minimum PDOP. As indicated by the graph, the “Best Time” grid produced by *Satellite Viewsheds* is not guaranteed to correspond with the time of maximum receiver accuracy. However, the time of maximum satellite visibility often corresponds to the time of minimum PDOP.

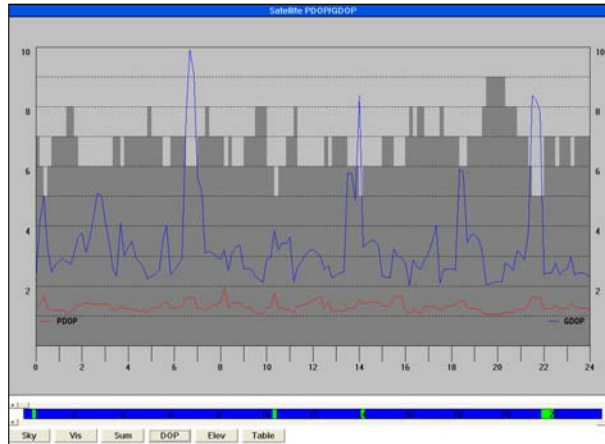


Figure 25. 24-hour GPS satellite visibility and PDOP predictions created by the *Satellite Availability Program*

3.5 Fresnel Zone Considerations

The final assumption in *Satellite Viewsheds* is that a cell must be able to establish direct LOS with a satellite for the satellite to be considered to be “visible” from the cell. In other words, the boundary between a visible zone and a shadowed zone on the output grid is a discrete 0/1, or “yes/no” boundary. This model is the same as an actual sun shadow of a building. In reality, a GPS receiver may continue to receive a signal even after it has moved into a shadowed area. Similarly, the receiver may lose reception even if it is slightly inside a “visible” zone on the map. The fuzzy boundary that exists in reality is created by signal effects like diffraction and also multipathing and reflection. While *Satellite Viewsheds* performs its analyses based on a Boolean visibility prediction, the effects of single knife-edge diffraction are considered in this section.

In this project, Fresnel zones were used to determine the likelihood of signal reception in shadowed areas. In Table 6 below, single knife-edge diffraction was used to calculate the width of the first Fresnel zone (F_1) for an obstruction at distances (d_2) of 50, 500, and 1000 meters from the receiver. The calculations were based on actual GPS look angles and ranges for Blacksburg, Virginia on a mid-March afternoon, for a signal wavelength of 0.1904 m:

Satellite	Az (deg)	El (deg)	Range, d_1 (km)	Distance to obstruction, d_2 (m)		
				50	500	1000
				F_1 (m)	F_1 (m)	F_1 (m)
PRN 03	309	27	22918	3.085	9.757	13.798
PRN 06	167	18	23508	3.085	9.757	13.798
PRN 15	295	55	21101	3.085	9.757	13.798
PRN 16	258	14	24436	3.085	9.757	13.798
PRN 18	239	73	20318	3.085	9.757	13.798
PRN 21	89	76	20102	3.085	9.757	13.798
PRN 22	239	40	20240	3.085	9.757	13.798
PRN 26	67	43	19828	3.085	9.757	13.798
PRN 29	51	32	20382	3.085	9.757	13.798

Table 6. Width of the first Fresnel zone for a typical GPS signal for a single knife-edge obstruction located 50, 500, and 1000 meters from the receiver.

The table clearly shows that the distance between a GPS receiver and an obstruction, such as a building or terrain edge, plays a major role in determining the width of the first Fresnel zone. With 50 m between the receiver and the theoretical knife-edge, the width of the first Fresnel zone is around 3 m.

The graph shown in Figure 26 provides a method for assessing the effect of the knife-edge diffraction on the signal. On the graph, diffraction loss of the signal, in decibels (dB), is plotted against the degree of blockage of the

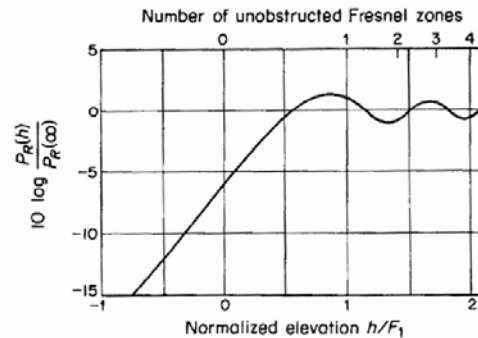


Figure 26. Diffraction loss in decibels for signal propagation paths with various clearances over a knife-edge obstacle (Livingston, 1970)

Fresnel zones. The graph shows that as the first Fresnel zone, or F_1 , becomes fully obstructed, the diffraction loss is about 6 dB. According to Dr. Timothy Pratt, an Affiliate Faculty Member of the Center for Wireless Telecommunications at Virginia Tech, GPS signals typically lose synchronization at a loss of about 4 dB (Pratt, personal communication, 2005). According to the graph, a diffraction loss of 4 dB occurs when h / F_1 (as shown on the diagram in Figure 27) equals about 0.2. When 50% of the first Fresnel zone is obstructed, or $h / F_1 = 0$, the LOS path is exactly grazing the edge of the obstruction. Using the results shown in Table 6 for a knife-edged obstruction 50 m from a GPS receiver, F_1 is about 3 m. Thus, for $h / F_1 = 0.2$, $h = 0.6$ m. Again, a GPS receiver is likely to lose reception at a diffraction loss of 4 dB, and that occurs when the LOS path is only 0.6 m above the corner of the obstruction. Therefore, *Satellite Viewsheds* assumes that reception is lost when the LOS path becomes obstructed, as shown in Figure 28. Based on the above analysis, the difference in predictability for incorporating or not incorporating Fresnel clearances is negligible.

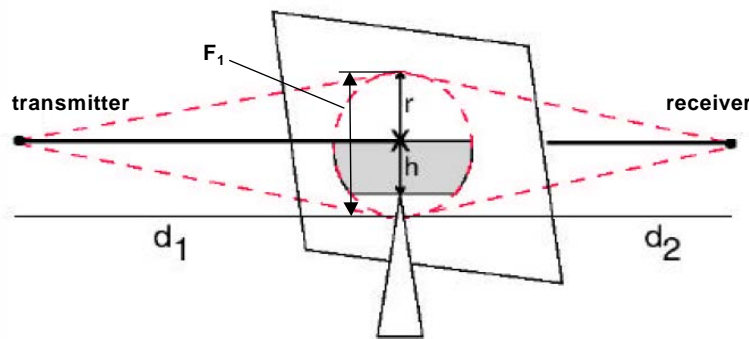


Figure 27. Schematic diagram illustrating first Fresnel zone clearance. The red dashed line represents the first Fresnel zone, and its radius is F_1 . The white triangle is the knife-edge obstruction that interferes with the first Fresnel zone. The distance from the LOS path to the obstruction is indicated by h (modified Baldassaro).

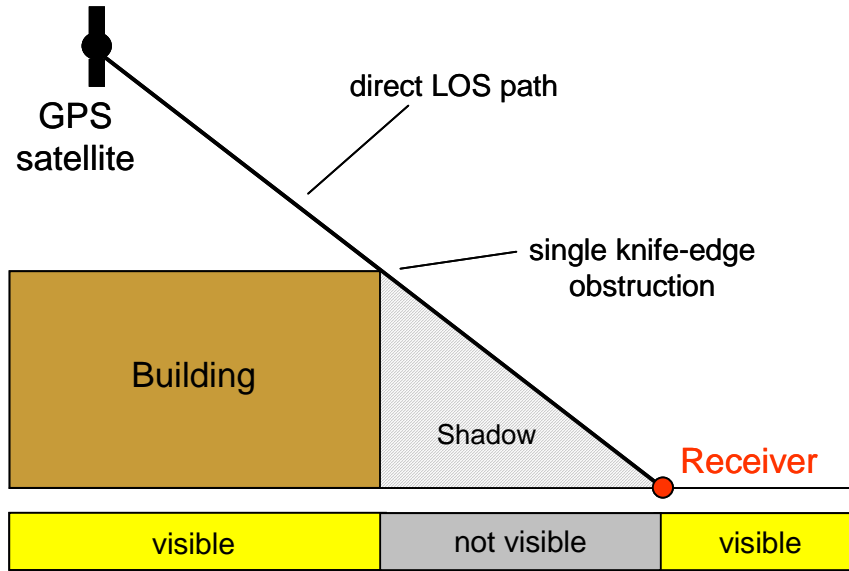


Figure 28. Illustration representing the assumption made by the satellite viewsheds tool that LOS contact must be established between the satellite and a cell for the cell to be considered visible

Chapter 4. Algorithm Design and Testing

This chapter is dedicated to the design of the *Satellite Viewsheds* program and to the methodology used to test its results. In the first section, the algorithm itself will be explained through a step by step description of the process. The descriptions are not meant to provide comprehensive explanations of the code line by line, but rather a procedural summary of the major algorithms. The code itself has been documented extensively line by line, allowing for any user or future researcher to obtain a more detailed explanation of the processes. The second section will describe how the program was used to predict satellite visibility on the Virginia Tech campus and the verification of the results.

4.1 Algorithm Design

Satellite Viewsheds runs in ArcGIS version 9, in the standard ArcMap window. The tool was written in the Microsoft Visual Basic for Applications (VBA) version

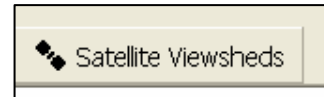


Figure 29. ArcMap button that loads *Satellite Viewsheds*

6.3 editor, included with ArcGIS. The program also references ArcObjects libraries. ArcObjects is an object-oriented programming language that was created by ESRI and is recognized by ArcGIS and supported by the VBA editor. To run *Satellite Viewsheds*, the user simply clicks on the ‘Satellite Viewsheds’ button with the small satellite icon, shown in Figure 29. Clicking on the button loads and displays the Satellite Viewsheds user form shown in Figure 18 (Chapter 3). The user form is the interface through which the user provides all input to the program. The input values, described in detail in Chapter 3, are

all restricted to legal inputs only. For example, the drop-down lists, or combo boxes, are only populated with legitimate values. The file inputs only allow the selection of .txt files for the TLES and .aux grid files for the surface model grid. In addition, a user must enter a numerical value between 0 and 90 for the horizon masking angle. It is difficult for a user to provide an erroneous value on the user form.

When the 'Run' button is clicked, the program opens the surface model grid, extracting and storing the grid's properties. The routine then determines whether any additional information from the user is required. Additional information is required only if:

- the user has specified a time zone that is not within the continental U.S.
- the user has requested to enter the z factor manually
- the coordinate system of the grid is not geographic, so the user must supply the latitude and longitude of the center of the grid
- the coordinate system of the grid could not be determined and the user is asked to supply both the z factor and the coordinates.


Next, the program determines the test time(s) provided by the user in GMT based on the time zone of the test area. To determine the test times for the time range option, the time difference between the initial and final test times is divided by the total number of tests specified by the user minus one to obtain the time interval between tests. The time interval is then added to the initial test time and the process is continued until the ending test time is reached. Thus, the test times are evenly spaced across the time range specified by the user. For each test time, the time of day is combined with the day of year to match the format of the epoch time, allowing for calculation of the time difference

between the epoch and test time. Next, the TLES text file is opened and the relevant data is extracted into arrays that are dimensioned by the total number of satellites in the element set. Once the information for all of the satellites is stored in arrays, the program loops through each satellite at each test time, calculating the look angle for each. The look angles are stored in an array dimensioned according to the number of satellites and number of test times. The primary result of all of these preliminary calculations is the look angle array, providing the azimuth and elevation for each satellite in the TLES at each test time.

Once the look angles for all satellites at all test times have been stored, the individual satellite viewsheds are created. The program loops through each satellite at each test time, creating viewsheds only for satellites with elevation angles greater than the user-specified horizon masking angle. The viewsheds are created using the Hillshade method; a member of ArcObject's ISurfaceOp interface. The program supplies the Hillshade method with the surface model grid as a GeoDataset, as well as the azimuth and elevation of the satellite, the z factor, and the specification required for the hillshade to be created with shadows modeled. In this manner, a viewshed grid is created for each satellite with cell values between 0 and 255. Cells that are assigned a value of zero are those cells that cannot establish LOS with the satellite. The individual satellite viewshed grid is then written to an array. A reclassification of the array is then performed, in which non-zero values in the array are changed to 1, creating an array with 0's for non-visible cells and 1's for visible cells. This process is demonstrated in Figure 30. At this

point, an array containing the viewsheds for each visible satellite at each test time is stored and ready for further manipulation.

221	220	0	0
151	27	89	0
36	201	0	0
5	0	0	194



1	1	0	0
1	1	1	0
1	1	0	0
1	0	0	1

Figure 30. Sample of hillshade array reclassification for a single satellite at a single test time for a 4 x 4 grid

After the individual satellite viewsheds array is created, the cell values in all viewsheds for each test time are added together and stored in array dimensioned by the number of test times. The array contains the total number of satellites visible from each cell at each test time.

4.1.1 Single Test Time

An example of the process is shown in Figure 31, in which there are three visible satellites at a single test time. If the user has chosen to perform the visibility prediction for a single test time only, the combined viewshed array is then stored into a raster dataset called the “Number of Visible Sats” array for descriptive purposes. The new grid depicting the number of satellites at every cell in the test area is then labeled and symbolized with a black to white color ramp and displayed on the ArcGIS screen (Figure 32 below). On the map, the black areas represent cells with the fewest visible satellites

1	1	0	0
1	1	1	0
1	1	0	0
1	0	0	1

+

0	0	0	1
1	0	1	1
1	0	0	1
1	0	0	1

+

1	0	0	1
0	1	1	0
0	1	1	1
0	1	0	1

=

2	1	0	2
2	2	3	1
2	2	1	2
2	1	0	3

Figure 31. Sample summation of individual reclassified hillshade arrays for three satellites at one test time for a 4 x 4 grid

and the white areas are those from which the highest number of satellites are visible. The grid is then saved in the folder specified by the user. Once in ArcMap after the program has finished running, the user is free to change the symbology of the grid if desired to meet his purposes.

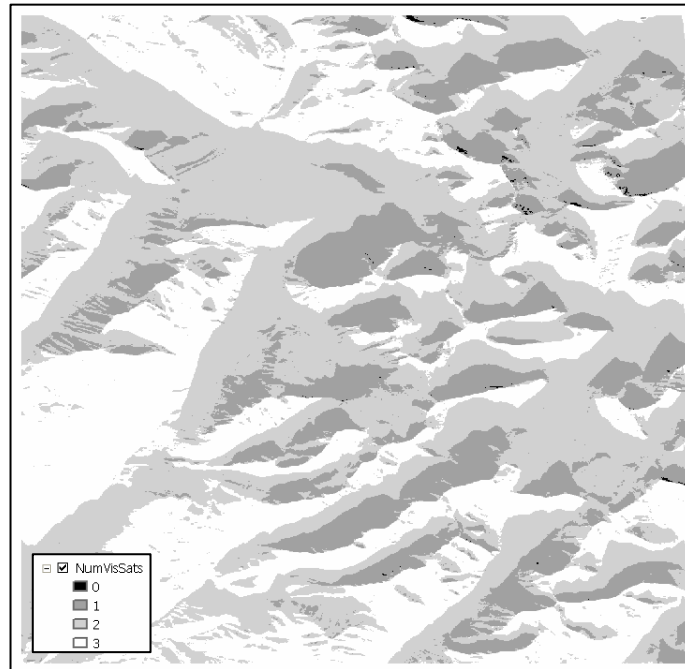


Figure 32. Sample *Satellite Viewsheds* visibility prediction for the Glacier DEM for 3 visible satellites using the 'Single test time' option

4.1.2 Multiple Test Times

If the user has selected to perform the satellite visibility predictions for a range of times, however, the grid in Figure 32 is not produced and the individual satellite viewshed array is passed on to the next procedure.

For visibility predictions across a range of times, the program loops through the combined viewshed array and populates a new array with the maximum number of

satellites visible at any of the test times for each cell, named the “Max Visible Sats” array for descriptive purposes. The time of maximum satellite visibility in each cell is also recorded into a new array, the “Best Time” array. The values in the Best Time array are actually integers representing the test times, with a “0” representing the initial test time. Next, the combined viewshed array containing the number of satellites visible at each time is re-examined to determine any cells that either have no satellites visible at any time or have the same positive number of satellites visible at all times. For cells in which there are never any satellites visible, a value of “-1” is assigned to the corresponding cell in the Best Time array. For cells in which there are the same positive number of satellites visible at all test times, a value of “999” is assigned to the corresponding cell in the Best Time array. Finally, the Max Visible Sats and Best Time arrays are written to new raster datasets, symbolized, and labeled. The Max Visible Sats grid is symbolized with a black to white color ramp in the same manner as the Number of Visible Sats grid produced for the single test time option. When the Best Time array is written to a grid, each cell is assigned an integer representing a time. Therefore, each class, or group of cells with the same value, is labeled with the proper time of day in local time according to their integer value, such as 6:53:00 PM. Cells that were assigned a value of “-1”, indicating that no satellites are visible at any of the test times, are labeled as “Never”. Cells that were assigned a value of “999”, indicating that the same positive number of satellites is visible at all of the test times, are labeled as “Anytime”. The Best Time grid is then symbolized with a random color ramp, and the user is free to change the symbology once the program has finished running. The grids are then saved in the folder specified by the user, and the grids are displayed automatically in the ArcMap window (Figure 33). Because the grids

were saved, they can be accessed at any time, even after removal from ArcMap. The program is also designed so that the original surface model grid of the test area is not changed in any way by the algorithm. After it is opened and the information is extracted, it is closed and remains unaltered. It is important to note that the Best Time grid does not convey satellite visibility across the entire test range, but only at the individual test times specified by the user. Therefore, it is up to the user to tailor the test time settings to his or her specific study.

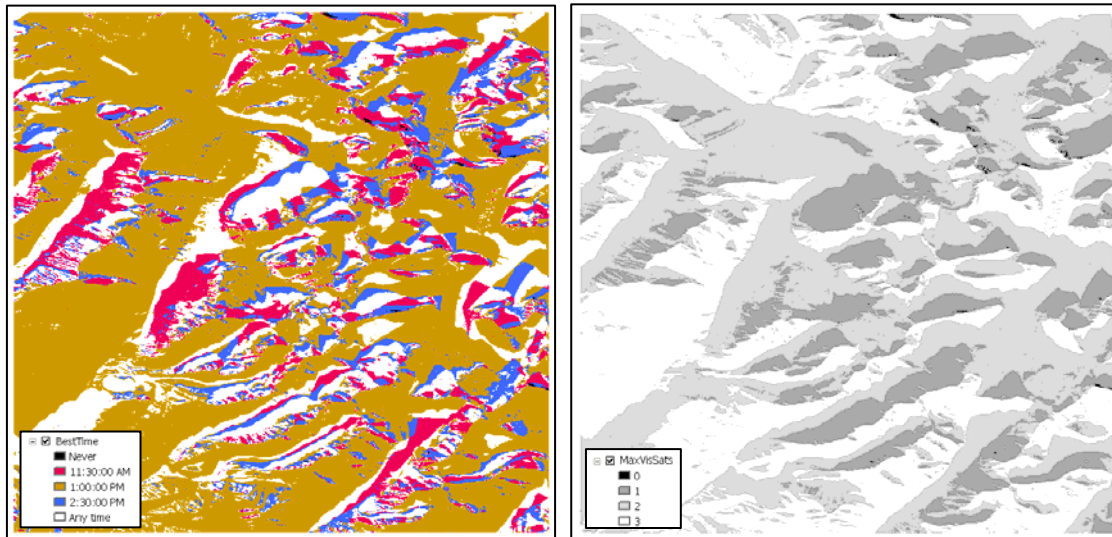


Figure 33. Sample 'BestTime' (left) and 'MaxVisSats' (right) grids of the Glacier DEM created by *Satellite Viewsheds* for the 'Time range' option using three test times from 11:30 AM to 2:30 PM, for three visible satellites

The final process of *Satellite Viewsheds* is to create a text file containing a summary of the program, if the user has elected to do so. The report file is given the name supplied by the user and is saved in the directory of the original surface model grid. The report file summarizes:

- all user inputs and the specifications of the surface model grid, including its coordinates, z units and z factor.

- for each test time, each satellite in the TLES and its elevation angle, azimuth angle, and percent coverage of the test area.
- the times used in the best times grid. If the user has performed the analysis across a range of times, the report provides a key for the values in the Best Time grid. Although the program automatically displays the grid with the proper labeling, the labels are lost if the user removes the grid and reloads it at a later time. The key lists each integer value in the grid and the time that it represents.

A sample program summary report is provided in Appendix A. After the report is written, the program finishes. At that point, the user may perform any desired raster operations supported by ArcMap with the new grid(s).

4.2 Program Testing Methodology

4.2.1 Theoretical Testing

To assess the accuracy of the look angle calculations performed by *Satellite Viewsheds*, they were compared with predictions made by WinOrbit, an industrial visibility tool. WinOrbit was written by Carl Gregory at the University of Illinois at Urbana, and is available for free online at www.sat-net.com/winorbit. Like *Satellite Viewsheds*, WinOrbit performs its calculations based on a TLES supplied by the user. The program can perform a multitude of calculations for various satellites for any time and location on earth, including ground tracking, satellite coverage areas and satellite-target relationships such as the range and look angle. In this study, a full GPS TLES was used to predict satellite look angles for the same target at the same time with both the new GIS tool and WinOrbit. In WinOrbit, the test was actually performed twice using

different orbital models for comparison purposes. The first test used the “SG4” orbital model, WinOrbit’s most accurate orbital model which does not make the assumptions used in *Satellite Viewsheds*, and thus accounts for effects of the sun and the moon, atmospheric drag, irregularities in the earth’s gravitational field, and elliptical orbits. While no orbital model is perfect, the SG4 model is the most accurate look angle prediction method available. The second set of WinOrbit look angle calculations were performed using WinOrbit’s “Ideal” orbital model, with the eccentricities of the orbits set to zero. Calculations performed using the “Ideal” model are similar to those performed by *Satellite Viewsheds*. The “Ideal” orbital model assumes that the earth is a point in space and that the sun, moon and other celestial bodies have no influence, meaning that each orbit is a perfect ellipse whose orientation in space is fixed. In addition, the second set of calculations was performed with the “Ignore Drag Terms” option selected. The look angle calculations of *Satellite Viewsheds* were compared with the predictions provided by the Ideal orbital model in WinOrbit. Using the SG4 model then provided a method of assessing the combined effects of the assumptions present in the calculations of the new tool.

4.2.2 Field Testing

In order to assess *Satellite Viewsheds*’s performance in a real-world scenario, the program was field-tested on the Virginia Tech campus (Figure 34). The objective of the test was to quantify



Figure 34. Aerial photograph of the Virginia Tech campus (photo by Rick Griffiths, courtesy of www.vt.edu)



Figure 35. Trimble GeoXT GPS receiver used for data collection during the field test

the tool's performance in not only predicting the number of visible satellites but also the location of those satellites in the sky. The first step in the testing process was the collection of the data. On two separate days, a Trimble GeoXT GPS receiver (Figure 35) was used to collect 44 points at stratified random locations across the Virginia Tech campus. On one day, the points were intentionally collected in the morning and on the other test day the points were collected in the afternoon. This staggering of the time

of day for the tests was to ensure that different satellites would be visible for each test day due to the 12-hour orbits of GPS satellites. The points were collected in areas where the sky was largely unobstructed and also in locations adjacent to buildings (Figure 36). Each point saved to the unit was actually an average of at least ten positional recordings taken with the receiver in the same location at an interval of one second. For each point, the time, PDOP, visible satellites and their look angles, all provided by the receiver, were recorded manually (Figure 37). After the points had been collected, they were imported from the receiver using Trimble's Pathfinder software. The points were then differentially corrected over the Internet using the Blacksburg base station located at the Virginia Tech Corporate Research Center. Post-processing differential correction uses a GPS receiver at a precisely known location to record errors in transmitted GPS signals. When collected data points are sent to the station, they are compared with the station's recordings and corrected accordingly, possibly producing points with sub-meter accuracy. After the data points had been differentially corrected, they were exported

from the Pathfinder software as an ArcGIS point shapefile. The locations of the points laid on top of the campus surface model grid can be seen in Figure 38.



Figure 36. Field test GPS points were recorded in both open areas and adjacent to buildings.

1			PDOP: 3.14
			Time: 10:31
Satellite	Elevation	Azimuth	
2	52	270	
4	67	21	
5	36	301	
10	19	195	
31	23	110	

Figure 37. Sample of one of 44 manual field test point recordings containing the point number, time, PDOP, visible satellites and their look angles

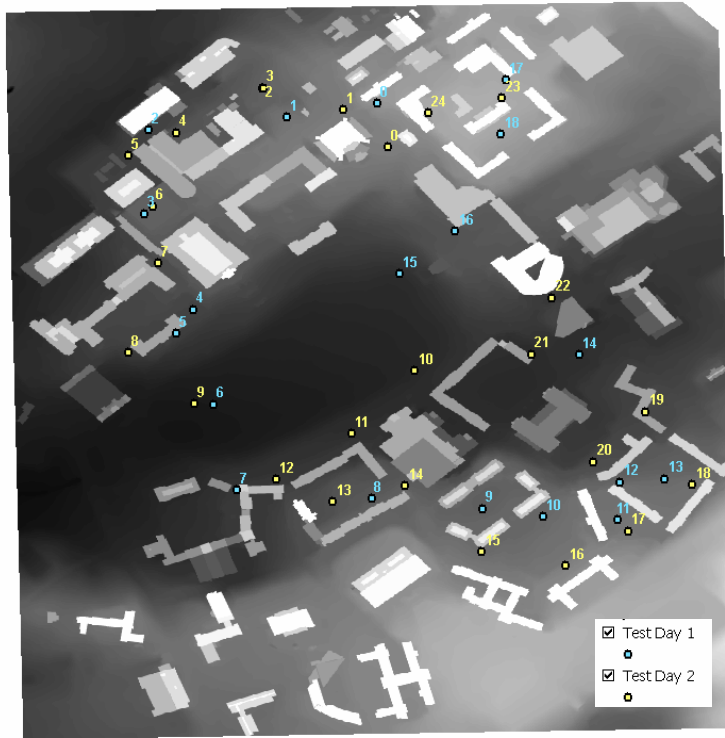


Figure 38. GPS points from both field test days laid on top of Virginia Tech surface model grid

The satellite visibility parameters observed at each test time were recorded for comparison with the predictions of *Satellite Viewsheds*. After the points were collected with the GPS unit, the tool was used to predict visibility at every time that a point was collected during the field test using the VT Campus 1-foot surface model. The tests were performed using the ‘Single test time’ option and the TLESs published the days of the field tests, which produced a grid depicting the predicted number of satellites visible from each cell in the grid at that time. After overlaying the field test points on to the satellite visibility prediction grid as shown in Figure 39, the total number of visible satellites as predicted by the program was visually determined and recorded. The process was repeated for all 44 field test points, allowing for comparison between the predicted and

observed number of visible satellites at each. (The table shown in Appendix B contains each field test point with its PDOP, observed number of visible satellites and predicted number of visible satellites.) In addition, the discrepancy between the observations and predictions was calculated, allowing for a simple statistical analysis of the difference. The mean and maximum of the set of differences were determined, as well as a frequency table of the set. Also, the assumption by *Satellite Viewsheds* that the time of maximum satellite visibility is also the time of optimal receiver performance, outlined in Section 3.4.7, was revisited. Using the table, the observed PDOP was plotted against the observed number of visible satellites to further examine the relationship between the two.

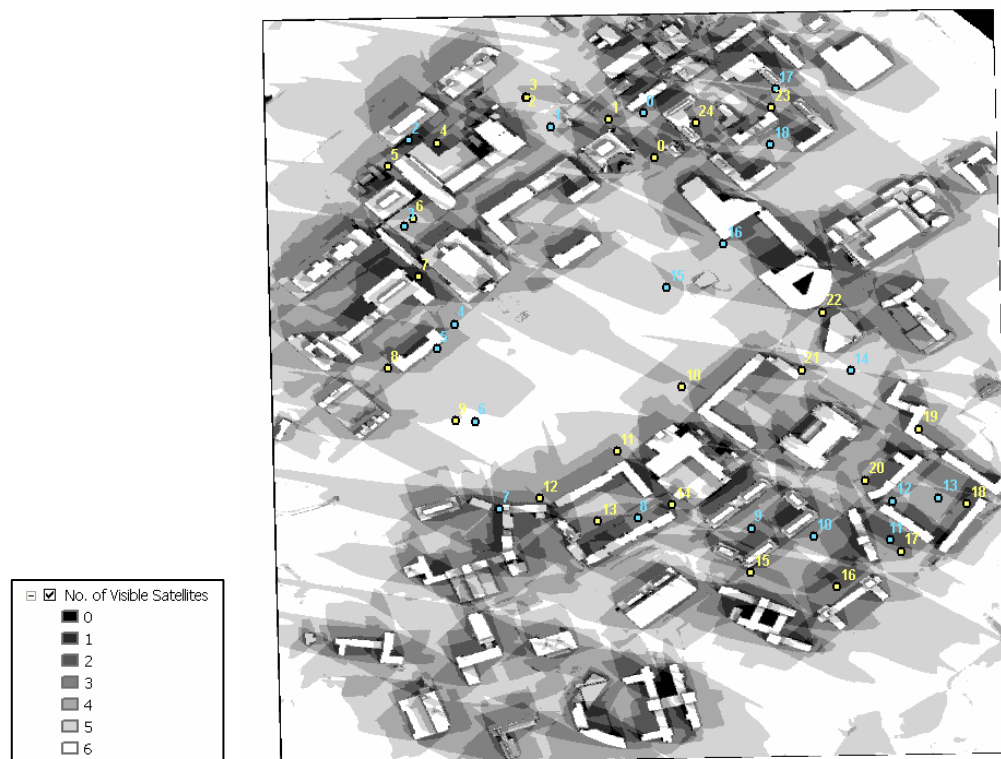


Figure 39. GPS test points laid on top of *Satellite Viewsheds*' predicted 'Number of visible satellites' grid for the Virginia Tech campus at 2:29 PM on April 11, 2005. A grid like this one was created for every GPS point recording time, allowing the prediction of the number of visible satellites for each.

For the 24 points collected on the second test day, a program summary report was also created for all *Satellite Viewsheds* predictions. In the reports, the predicted azimuth and elevation angles for each satellite were provided for each test time. Using the reports, the table shown in Appendix C was created. For each observed satellite at each field test point on Day 2 (125 samples), the table contains the observed and predicted look angles as well as two fields containing the difference between them. It is important to note that the term “observation” here actually refers to azimuth and elevation angles *predicted* by the Trimble GPS receiver. The receiver does not observe the satellites’ positions, but performs high-level calculations to determine where the satellites should be. Sophisticated equipment is required to determine the actual, observed look angle of a celestial body. However, the values predicted by the receiver, termed “observations” here, are the most accurate predictions readily available.

Chapter 5. Results

5.1 Look Angle Computation Verification Against a Standard Program

As discussed in Chapter 4, GPS satellite look angles predicted by *Satellite Viewsheds* were compared with look angles calculated by WinOrbit. Both the “Ideal” and SG4 orbital models were used to calculate look angles in WinOrbit (designated WO in Table 9 below), with the “Ideal” model using essentially the same assumptions as *Satellite Viewsheds*. The SG4 calculations were used to assess the combined effect that all of the assumptions have on the accuracy of the look angle calculations. Table 7 shows predictions for the full GPS constellation at 22:00 GMT on March 20, 2005 in Glacier National Park, Montana. Although both programs provide look angles for both visible

Satellite	WO (e>0, drag, SG4)		WO (e=0, no drag, Ideal)		Satellite Viewsheds	
	Az (deg)	El (deg)	Az (deg)	El (deg)	Az (deg)	El (deg)
PRN 03	309	27	310	26	309.8	26.4
PRN 06	167	18	167	18	166.9	17.8
PRN 15	295	55	296	56	295.7	56.1
PRN 16	258	14	258	14	257.8	13.6
PRN 18	239	73	239	74	238.3	73.7
PRN 21	89	76	90	75	90.2	74.6
PRN 22	239	40	239	40	238.4	39.6
PRN 26	67	43	68	44	68.3	44.2
PRN 29	51	32	51	32	51.1	32.4

Table 7. Comparison of look angle calculations by WinOrbit’s SG4 model, WinOrbit’s Ideal model, and *Satellite Viewsheds* for all visible satellites at 22:00 GMT on March 20, 2005 in northwestern Montana

and non-visible satellites, only the visible satellites are shown in the table. The largest discrepancy between the predictions of *Satellite Viewsheds* and the WinOrbit predictions is 1°. In fact, of the 18 look angles compared, only two of *Satellite Viewsheds*’ predictions did not match WinOrbit’s predictions using the “Ideal” orbital model. These small differences between the *Satellite Viewsheds* and the WinOrbit “Ideal” calculations

are most likely attributable to slightly varied assumptions in the orbital models used. The table also shows the combined effect of the assumptions made by *Satellite Viewsheds*, including using circular orbits, ignoring drag and the earth's irregular gravitational field, treating the problem as a two-body problem. The assessment was based on the SG4 model, the most accurate orbital prediction model available. The table clearly shows that the effect of the assumptions on the look angle predictions is relatively minor. Table 8 shows a summary of the comparison of the look angles calculated by *Satellite Viewsheds* and WinOrbit's "Ideal" and SG4 models. To summarize the look angle verification test, the calculations performed by *Satellite Viewsheds* match almost perfectly to predictions provided by an industrial tool. In addition, the assumptions used by the tool to simplify the look angle calculation algorithm resulted in only minor errors. The look angle predictions are comparable to those obtained from the best method currently available.

	Discrepancy (degrees)		
	-1	0	1
WinOrbit Ideal model:	2	16	0
WinOrbit SG4 model:	4	7	7

Table 8. Frequency table of discrepancies between 18 look angles predicted by *Satellite Viewsheds* and predictions of WinOrbit's "Ideal" and SG4 orbital models.

5.2 Field Test Results

5.2.1 Number of Visible Satellites

The field test on the Virginia Tech campus revealed that the *Satellite Viewsheds* program is able to accurately and consistently predict GPS satellite visibility. The number of visual satellites observed at the 44 field test points was compared with the predicted number of visible satellites for the same times and locations, using the surface

model grid of the campus.

The complete comparison

table is shown in Appendix C.

Table 9 shows the results of

Mean discrepancy (satellites)	-0.023
Maximum difference (satellites)	1
Frequency of discrepancy = +1 satellite	3/44 (~6.8%)
Frequency of discrepancy = -1 satellite	4/44 (~9.9%)
Frequency of no discrepancy	37/44 (~84.1%)

Table 9. Statistics of data set containing discrepancy values between observed and predicted number of visible satellites

the comparison between the observed and predicted visible satellite counts. For just over 84% of the 44 test points, *Satellite Viewsheds* correctly predicted the number of visible satellites for the time of data collection. At no time were the program's predictions in error by more than one satellite. *Satellite Viewsheds* over-predicted by one satellite for four test points and under predicted by one satellite for three test points. For this sample data set, the program slightly tends to under predict the number of satellites that can be seen from a given point for a given test time. The slight under prediction is most likely a result of the occurrence of multipathing in the field. At the under predicted points, it is likely that the receiver collected data from a satellite whose signal had been reflected while the satellite was not considered visible by *Satellite Viewsheds* because direct LOS was not established. The over predictions are likely a result of possible signal obstructions in the field that were not included in the Virginia Tech campus surface model grid, such as trees. The discrepancies are also possibly a result of slightly erroneous look angle calculations by *Satellite Viewsheds* due to its inherent assumptions.

In addition to the summary statistics, *Satellite Viewsheds*' ability to predict the number of visible satellites was examined through the creation of an error matrix. The error matrix, shown in Table 10, contains the number of correctly and incorrectly classified satellites (24 total satellites for each of the 44 test times). The diagonal of the

error matrix contains the number of satellites predicted visible by *Satellite Viewsheds* and the number that were actually visible in the field; as well as the number of satellites that were predicted to be not visible and actually were not. The number of incorrectly predicted satellites is shown in the two cells off of the diagonals.

		Observed	
		Visible	Not Visible
Predicted	Visible	238	4
	Not Visible	3	811

Table 10. Error matrix comparing satellite visibility as predicted by *Satellite Viewsheds* and the field observations, with the diagonal containing correctly predicted satellites.

The k-hat, or kappa (κ), of the error matrix was then calculated. The kappa test provides a measure of the contribution of chance agreement to the success of the predictions (Campbell, 2002):

$$\kappa = \text{observed} - \text{expected} / (1 - \text{expected}) \quad \text{Eq. 5.1}$$

A kappa value of +1.0 means that a classification is perfectly effective, with no contribution from chance agreement. A kappa value of 0 indicates that the success of the classification is the same as it would be if the values were randomly classified. Using a Visual Basic script written by Dr. Bill Carstensen of the Virginia Tech Department of Geography, the kappa of the error matrix shown above was determined to be 0.981, with a significance level of 0.05. This means that the visibility predictions of *Satellite Viewsheds* were almost perfectly effective, with very little contribution from chance agreement. The kappa value of 0.981 means that the results of the prediction are 98.1% better than would be expected from chance predictions. The significance level indicates that one can be confident that less than one out of every 20 predictions is subject to

chance error instead of systematic errors. Also, because the data set is statistically significant, the results of the comparison can be expected to represent any test performed under similar conditions.

Although the issue of PDOP versus number of visible satellites as receiver performance indicators was addressed in Chapter 3, the field test provided another opportunity to examine their relationship. *Satellite Viewsheds* does not predict PDOP, but the field test data provided further evidence that the time of maximum number of visible satellites is also the time of the optimal PDOP. The graph in Figure 40 shows observed PDOPs plotted versus the observed number of visible satellites. Although there are several outlying data points, the graph clearly shows the tendency of a decrease in PDOP with an increase in number of visible satellites. If the clusters of PDOP values for each visible satellite value are examined, they strictly follow the tendency. Also of note is the sharp increase in PDOP values from five visible satellites to four.

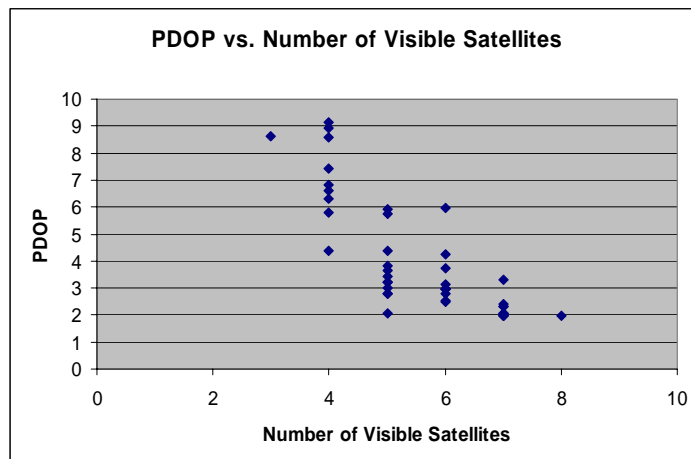


Figure 40. Observed PDOP versus observed number of satellites for 44 field test points

5.2.2 Look Angle Computation Verification against GPS field Data

The 125 look angles predicted by *Satellite Viewsheds* for the times of the field test point recordings were compared with the observed values. The differences between the observed and predicted look angles were calculated and are shown in the table in Appendix C. Using the table, simple statistics were calculated on the discrepancy fields; including the mean, maximum and frequency distribution. The summary statistics are shown in Table 11. The mean of the azimuth angle discrepancy set was 0.360° and the standard deviation of the set was 0.928°. The mean of the elevation angle discrepancy set was 0.576° and its standard deviation was 0.663°. The lower standard deviation of the elevation discrepancy set implies that the individual values are less likely to deviate from the mean discrepancy. In other words, for this particular test, the predicted elevation values are more precise and consistent than the predicted azimuth values. Also, it was observed that the maximum and minimum values for the entire set of discrepancies was 2° and -2°, respectively.

Discrepancy Set Statistics (degrees)				
	Mean	Minimum	Maximum	Std. Dev.
Azimuth	0.36	2	2	0.93
Elevation	0.58	-1	2	0.66

Table 11. Summary statistics of discrepancies between look angle predictions by *Satellite Viewsheds*

Table 12 was then created containing the frequency distribution of the discrepancy values for both azimuth and elevation. The graph in Figure 41 shows the frequency distribution of the discrepancy classes of the predictions. The graph indicates that a vast majority of the predictions were within 1° of the observed values. Next, a X^2

(chi-squared) test was applied to the discrepancy sets to determine the nature of the discrepancies. The minimum and maximum discrepancy values of -2° and 2°

	Discrepancy					
	-2	-1	0	1	2	Total
Azimuth	5	12	53	43	12	125
Elevation	0	3	56	57	9	125
Total	5	15	109	100	21	250

Table 12. Frequency of each class of discrepancy between the observed and predicted azimuth and elevation angles

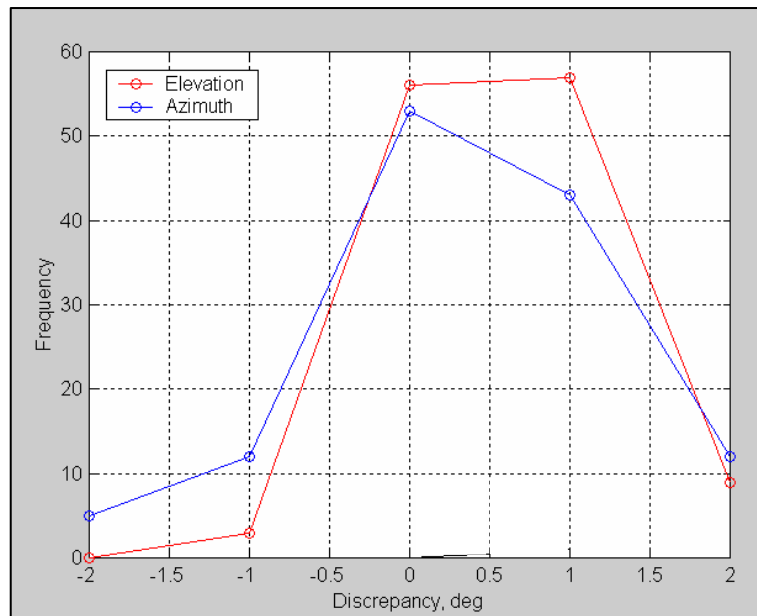


Figure 41. Frequency distribution of discrepancies between predicted and observed look angles.

respectively, dictated 10 classes (-2° , -1° , 0° , 1° , 2° for each angle). In the X^2 test, each of the ten classes of observations (χ_i) with mean, μ , and standard deviation, σ , was standardized as z_i by Equation 4.1 (Davis, 2002):

$$z_i = (\chi_i - \mu) / \sigma \quad \text{Eq. 4.1}$$

The standardized values of each z_i were then squared and summed, producing the X^2 value for the data set. Additional information regarding the methodology for determining

the X^2 value of the tabularized data is outlined in Connor-Linton, 2003. The X^2 value was then used to determine the significance level, α , of the data set, which describes the confidence that one may have that the discrepancies are systematic and *not* attributable to random error. Given the X^2 value and the degrees of freedom of the data set (4 in this case), the significance level was determined from Table 13, which lists critical values of X^2 for different degrees of freedom and selected levels of significance. The critical values represent the minimum X^2 value of a data set for which that set may be considered statistically significant. Most importantly, a statistically significant data set means that the pattern found in the data can be generalized to the larger population represented by the sample data set.

No. of Degrees of Freedom, ν	Significance Level, α				
	0.20	0.10	0.05	0.025	0.01
1	1.64	2.71	3.84	5.02	6.63
2	3.22	4.61	5.99	7.38	9.21
3	4.64	6.25	7.81	9.35	11.34
4	5.99	7.78	9.49	11.14	13.28
5	7.29	9.24	11.07	12.83	15.09
6	8.56	10.64	12.59	14.45	16.81
7	9.80	12.02	14.07	16.01	18.48
8	11.03	13.36	15.51	17.53	20.09
9	12.24	14.68	16.92	19.02	21.67
10	13.44	15.99	18.31	20.48	23.21

Table 13. Critical values of X^2 for various degrees of freedom and selected levels of significance (Davis, 2002)

The X^2 value of the data set was determined to be 12.871. From the table in Davis, for 4 degrees of freedom, a X^2 value of 12.871 falls between the critical X^2 values of 11.14 for a significance level of 0.025 and 13.28 for a significance of 0.01. This means that the data set is significant to at least 0.025; or, that the characteristics of this data set can be assumed to represent the behavior of all data collected under similar

conditions. Also, a significance level of 0.025 means that for these test conditions, a user can be confident that at least 97.5% of the discrepancies are due to systematic error, and are *not* attributable to random effects.

Although the statistics discussed above are specific to the field test performed on the Virginia Tech campus, there is no reason to believe that their implications do not represent *Satellite Viewsheds*'s performance under any conditions. The discrepancies between the predicted and observed look angles are relatively minor and are unavoidable considering the assumptions made by the program in the calculations. The errors that do exist in the predictions are most likely attributable to the assumptions made in the calculations as well as the time difference between the exact time of point recording and the time entered into *Satellite Viewsheds* for the predictions. While the field test points were recorded in real time, *Satellite Viewsheds* accepts test times expressed in integer minutes. For GPS satellites that move more quickly across the sky (up to 30° per hour), the time difference may be sufficient to cause a small discrepancy between the predicted and observed look angles. Other rounding errors and possibly multipathing may also contribute to the discrepancy, but the differences most likely arise from the assumptions made by *Satellite Viewsheds* and the time difference between the field test and visibility predictions.

6.1 *Satellite Viewsheds*

A new, end-to-end GPS satellite visibility tool that considers LOS obstructions has been created for ArcGIS. Currently, no tools exist that predict GPS satellite availability based on local features in the receiver's environment that can block signals and cause problematic service. Of those that make some attempt to do so, no tools perform predictions for an entire area; instead they restrict their analyses to single points on the earth's surface. *Satellite Viewsheds* allows a user to predict the performance of his or her GPS receiver for an entire test area at any location and time with minimal user interaction. *Satellite Viewsheds* produces maps that show the user how many satellites will be visible at a test time and the time at which the most satellites will be visible across a time range. The program performs its predictions independently for each cell in the grid, providing the user with a visibility map at the resolution of his or her raster surface model grid. Because GPS receiver performance depends on the number of satellites with which it can establish an unobstructed LOS, the maps produced by the program allow a user to set-up data collection times and locations accordingly.

Satellite Viewsheds is unique in its ability to perform GPS satellite visibility predictions for an entire area while considering the effects of features in the local environment. The tool is user-friendly and includes many features that allow for its widespread use by GPS customers with varied objectives. Some of the key features of the program are listed below:

- The program accepts any valid raster surface model grid representing any portion of the earth's surface. The program accommodates grids with any units and any coordinate system. If the program encounters a problem determining the grid's coordinate system, it simply asks the user to specify the coordinates and z factor.

- The main user form updates dynamically as the user enters input values. For example, if the user selects February for the test month, the program only allows the selection of a value between one and 28 for the test day. In this manner, there is little chance for errors resulting from user entries. In addition, when the 'Run' button is clicked, the program extensively inspects the inputs to ensure that they are acceptable. For further assistance, the Help button on the form provides information about each of the user entries.

- Resulting satellite visibility maps are automatically displayed on the screen, complete with symbology and labeling. The grids are also saved permanently with a Value Attribute Table, which allows for any additional mathematical operations, such as manual reclassification or overlay, to be performed on the grid. The output grids also inherit all spatial reference properties of the user's surface model grid.

- The optional text report generated provides a summary of the test, including all inputs and parameters, as well as the look angles and percent coverage of the test area for every satellite in the TLES at each test time.

- The program accepts Two Line Element Sets (TLES) text files exactly as published by NORAD, meaning that the user does not need to manipulate the file in any way. For GPS satellites, the program extracts the name of the satellite, such as "PRN 01", for publishing in the program summary report.

- *Satellite Viewsheds* runs on any computer with a working copy of ArcGIS version 9, from any directory. The data supplied by the user may also reside in any location on the computer.

6.2 Future Research

While *Satellite Viewsheds* is fully-operational and achieves the objective of this research, there are several possible improvements for the tool that may be explored by future researchers. Perhaps the most pressing improvement for *Satellite Viewsheds* would be to eliminate some or all of the assumptions outlined in Chapter 3. To achieve greater accuracy in the satellite look angle calculations, a more accurate orbital model can be applied. The assumption that the GPS satellites are in circular orbits should be eliminated, along with the omission of the effect of atmospheric drag and the gravitational pull of other celestial bodies besides the earth. These improvements would not only enhance the accuracy of the predictions, but would also allow for visibility analysis of non-GPS telecommunications satellites, such as satellite radio and television. Currently, *Satellite Viewsheds* produces viewsheds for any satellite, but the user must examine the TLES of the satellite(s) to ensure that the eccentricity is close to zero. This assumption is close for GPS satellites, but may not be for all others.

A second enhancement that would prove worthwhile is that the satellite geometry could be used to calculate the PDOP at each cell in the grid, allowing the user to predict exactly how his or her receiver will perform at each location. *Satellite Viewsheds* provides the user with the number of satellites that will be visible at a given time and location. Although the number of visible satellites for a receiver is a reliable indicator of

receiver performance, PDOP calculations would serve as a 100% reliable indication of the accuracy of data collection.

A third avenue for future research would be to include GPS signal behavior in the actual program. In addition to the Fresnel zones discussed in this report, a future researcher may consider a method of modeling spatial components of signal reflection, refraction, or multipathing. If these phenomena could be incorporated into the program, a user would be able to predict the locations in which their receiver is likely to record erroneous positional information. In order to map signal behavior, the program would need to obtain the physical properties of the signal from the user. In this manner, the program could be used to assess visibility for any type of telecommunications satellite.

The surface models used in this research included solid terrain features, such as landforms and buildings. The program was not tested in areas in which possibly transparent obstructions exist. In many cases, a GPS receiver's performance depends not only on solid signal obstructions but is also influenced by obstructions through which signal may be partially transmitted or altered, such as vegetation. While the use of LiDAR data as the input surface model grid would allow the inclusion of features such as trees, they still cannot be treated as solid obstructions because they allow passage of signals in some cases. The best way to handle this issue may be alter the program to use 3-D vector data that contains an attribute with signal transmission properties.

Future research could also include the elimination of the assumptions involving the surface model grid, such as the omission of earth curvature, calculation of the look angles with the elevations of the cells set to zero, and the same look angles for every grid in the cell. While the effects of these assumptions were proven to be extremely insignificant for a large scale test area, their inclusion in the algorithm will result in more accurate satellite visibility predictions for analyses across large test areas.

Satellite Viewsheds met and exceeded the initial objectives of this project, but small improvements may provide an opportunity for commercial production and marketing. The computer code of the program itself was written with this intention in mind, and the program's extensive commenting and segmentation will allow a future researcher to improve only the relevant operations while the rest of the algorithm remains intact.

6.3 Conclusion

In recent years, both GPS and GIS have developed into predominant mapping tools with unlimited potential for future development. *Satellite Viewsheds* provides a powerful link between the two, using the powerful operations of GIS to optimize the capabilities of GPS. The ability to predict GPS satellite visibility provides a method of predicting GPS receiver performance because a receiver's functionality depends on the number of satellites from which it can acquire signals. Before the creation of *Satellite Viewsheds*, GPS users had no way of incorporating local signal obstructions into satellite visibility predictions for an entire test area. Current tools in the industry perform

predictions for single points on the earth's surface only; and consideration of local features that may obstruct GPS signals, such as buildings and terrain, requires a preliminary survey of the test site. *Satellite Viewsheds* eliminates the need for preliminary observation of a test site by using a surface grid to model the local environment. The program performs predictions for any location on earth for any test time or range of times. *Satellite Viewsheds* requires only the surface model grid and a TLES describing the orbits of the GPS satellites. If a user opts to perform a single test time analysis, the program produces a grid showing the number of satellites visible from each cell in the grid. If the user opts to perform the predictions for a range of times, two grids are produced: one showing the maximum number of satellites visible across the time range and another containing the time at which the maximum number of satellites is visible. A user can perform a full visibility prediction in a matter of minutes.

Satellite Viewsheds allows GPS users to predict and avoid times and locations at which their receiver will experience diminished service. Predicting receiver performance will maximize the efficiency of GPS data collection, saving time and money by allowing a GPS user to tailor his or her data collection routine to times and locations of optimal receiver performance.